The Bright Extragalactic ALMA Redshift Survey (BEARS) II:

Millimetre photometry of gravitational lens candidates

George J. Bendo
UK ALMA Regional Centre Node
The University of Manchester

Through a combination of peripheral involvement on the H-ATLAS Survey and work as an ALMA Contact Scientist, I became involved in a project initially led by Stephen Serjeant (now including Sheona Urquhart, Tom Bakx, and Masato Hagimoto) to measure spectroscopic redshifts for gravitational lens candidates identified in H-ATLAS data.

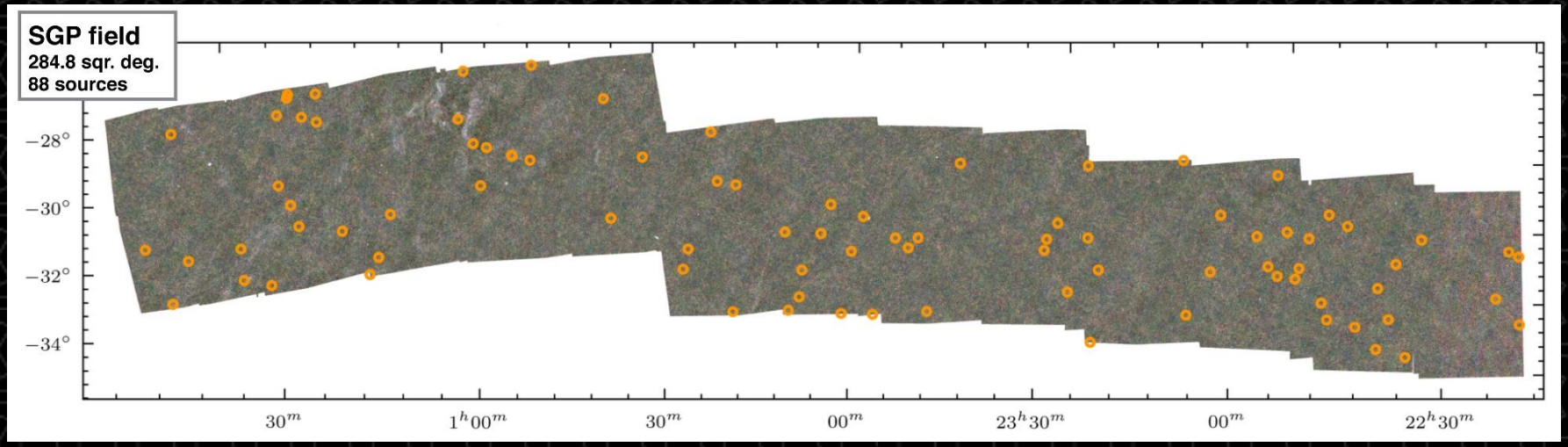

Bakx et al. (2018, MNRAS, 473, 1751)

This involved using spectral scans that eventually covered most of ALMA Bands 3 and 4. I thought it would be entertaining to use all of the excess data to make some continuum measurements.

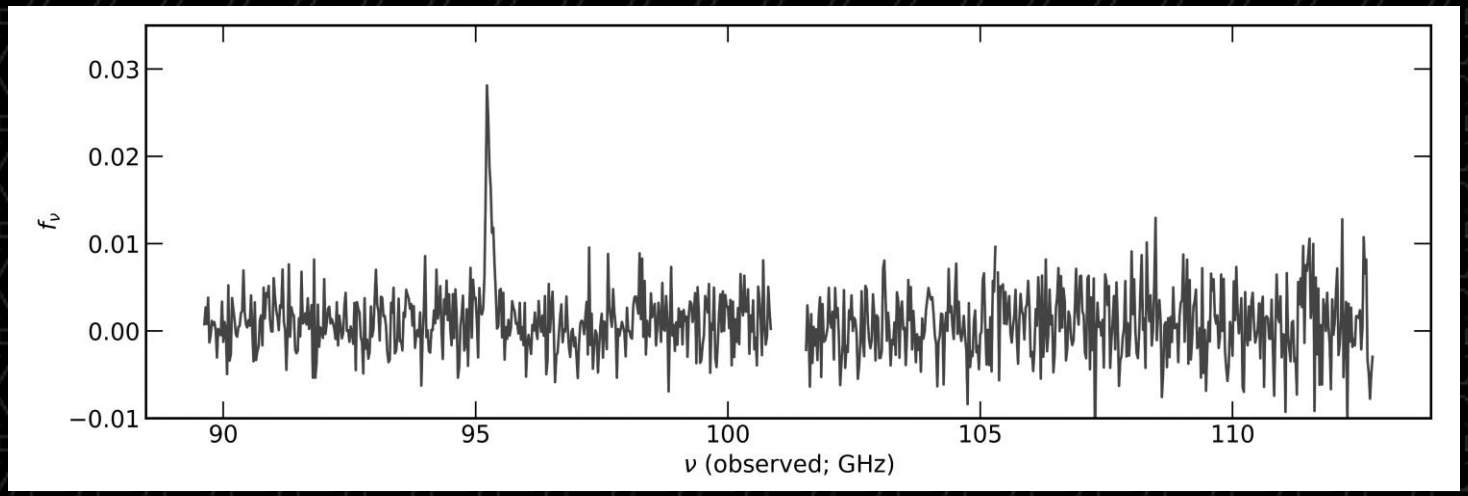

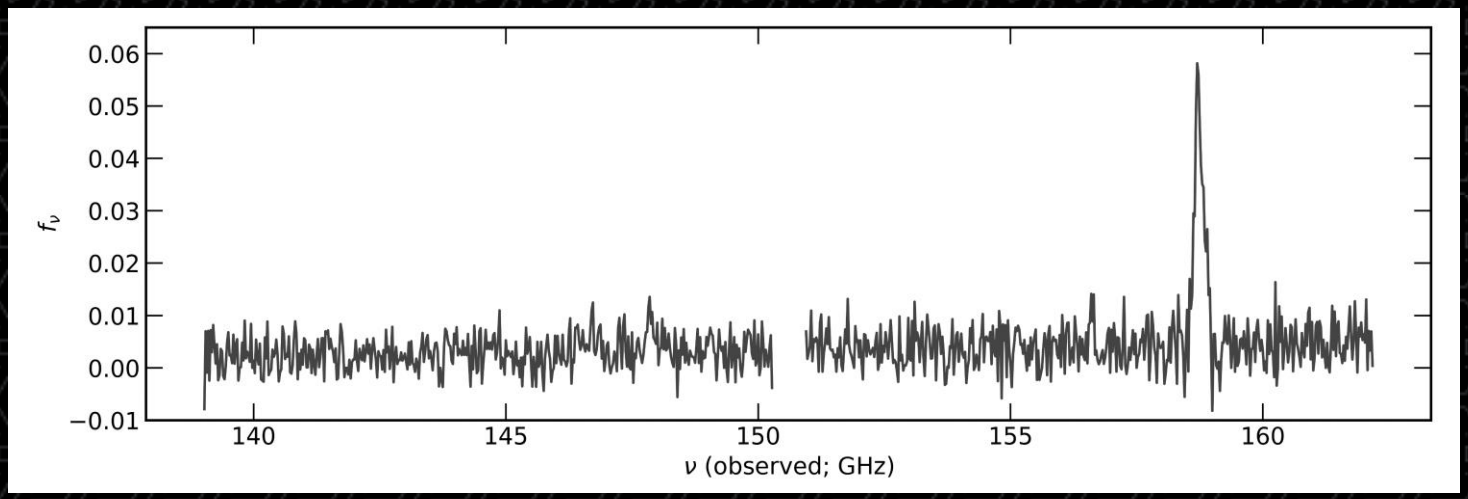

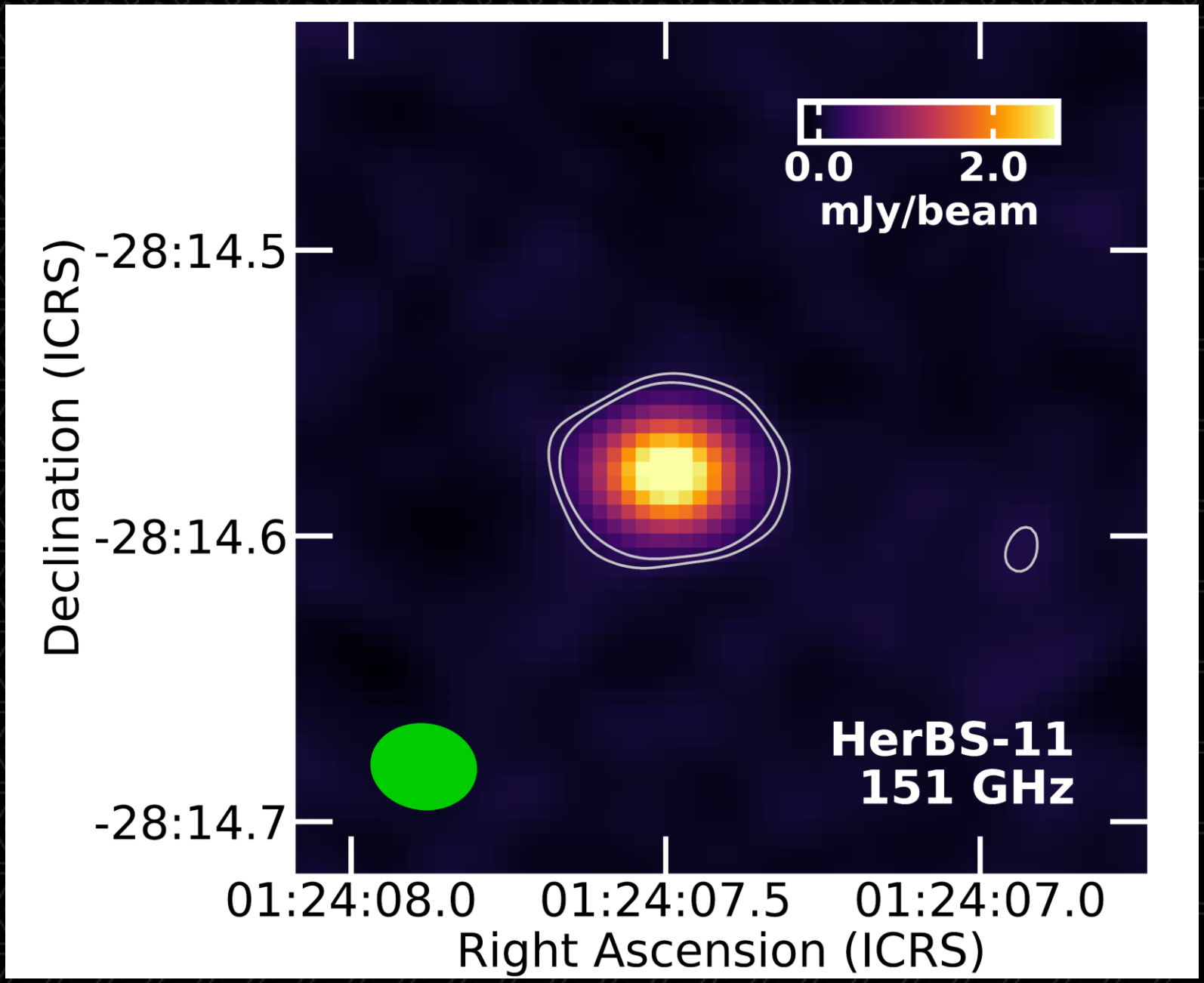
0.0
2.0
mJy/beam
HerBS-11
151 GHz
Declination (ICRS)
-28:14.5
-28:14.6
-28:14.7
01:24:08.0
01:24:07.5
01:24:07.0
Right Ascension (ICRS)

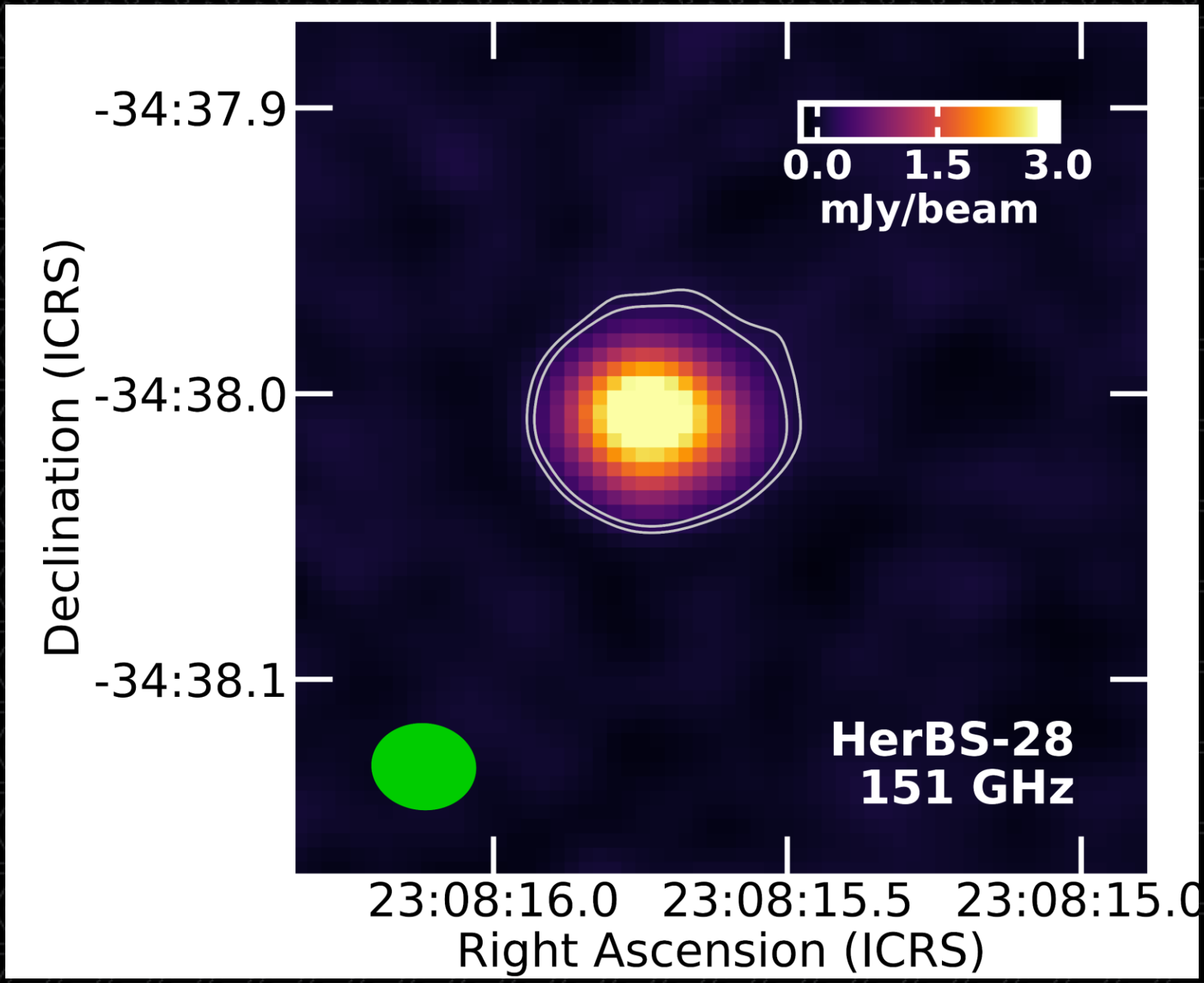
-34:37.9
-34:38.0
-34:38.1
Declination (ICRS)
0.0
1.5
3.0
mJy/beam
HerBS-28
151 GHz
23:08:16.0
23:08:15.5
23:08:15.0
Right Ascension (ICRS)

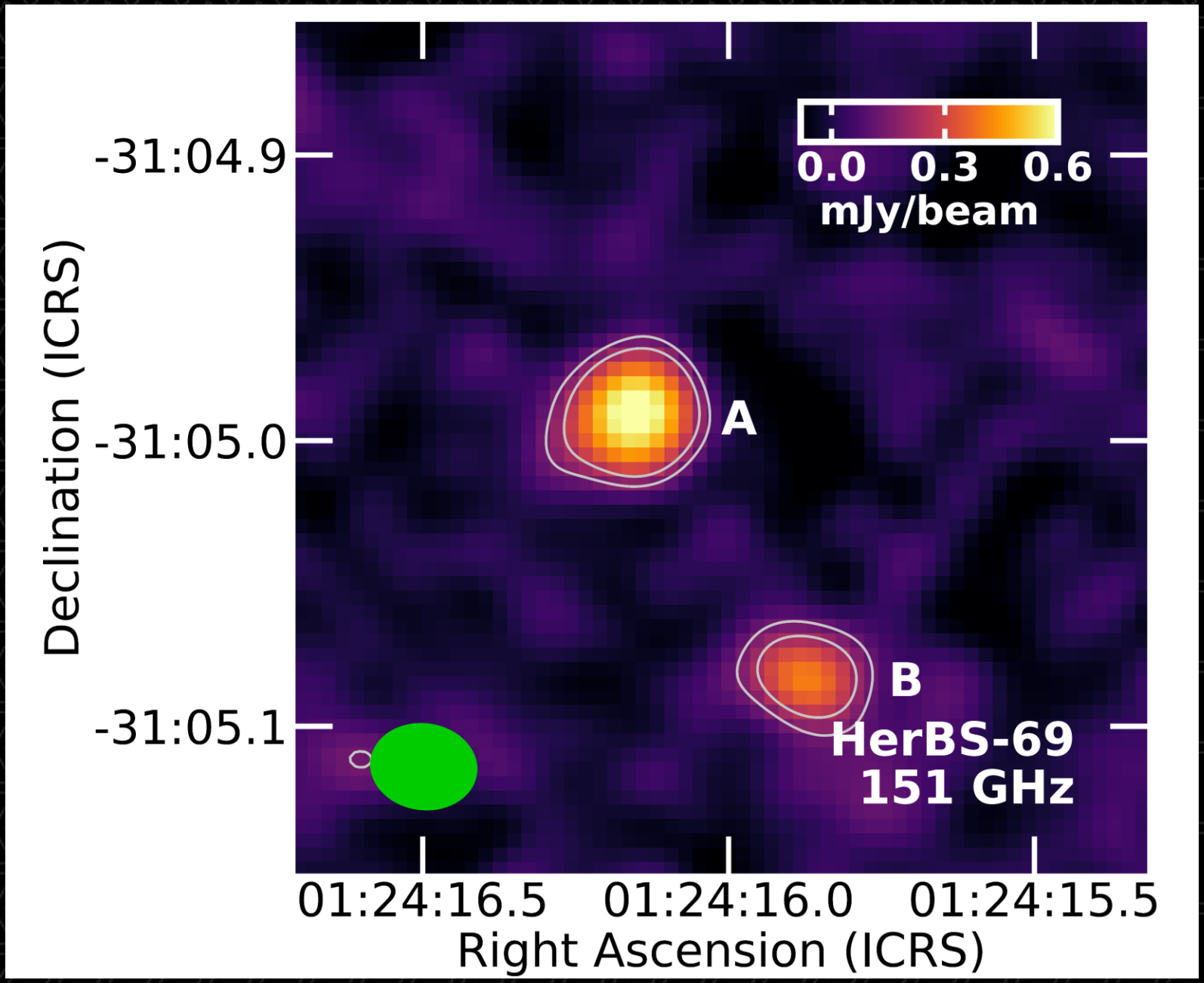
-31:04.9
-31:05.0
-31:05.1
Declination (ICRS)
0.0 0.3 0.6
mJy/beam
A
B
HerBS-69
151 GHz
01:24:16.5
01:24:16.0
01:24:15.5
Right Ascension (ICRS)

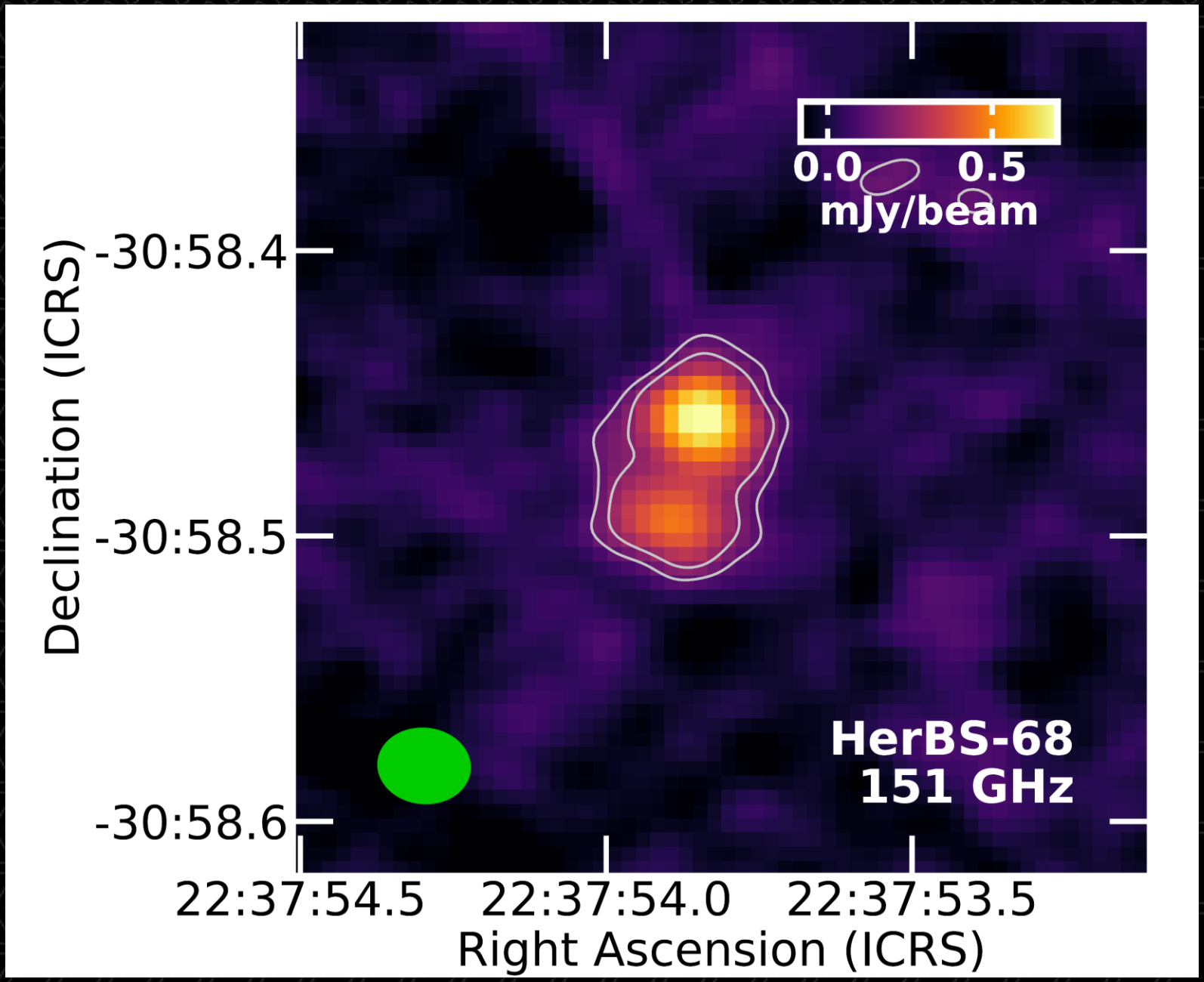
0.0
0.5
mJy/beam
HerBS-68
151 GHz
-30:58.4
-30:58.5
-30:58.6
Declination (ICRS)
22:37:54.5
22:37:54.0
22:37:53.5
Right Ascension (ICRS)

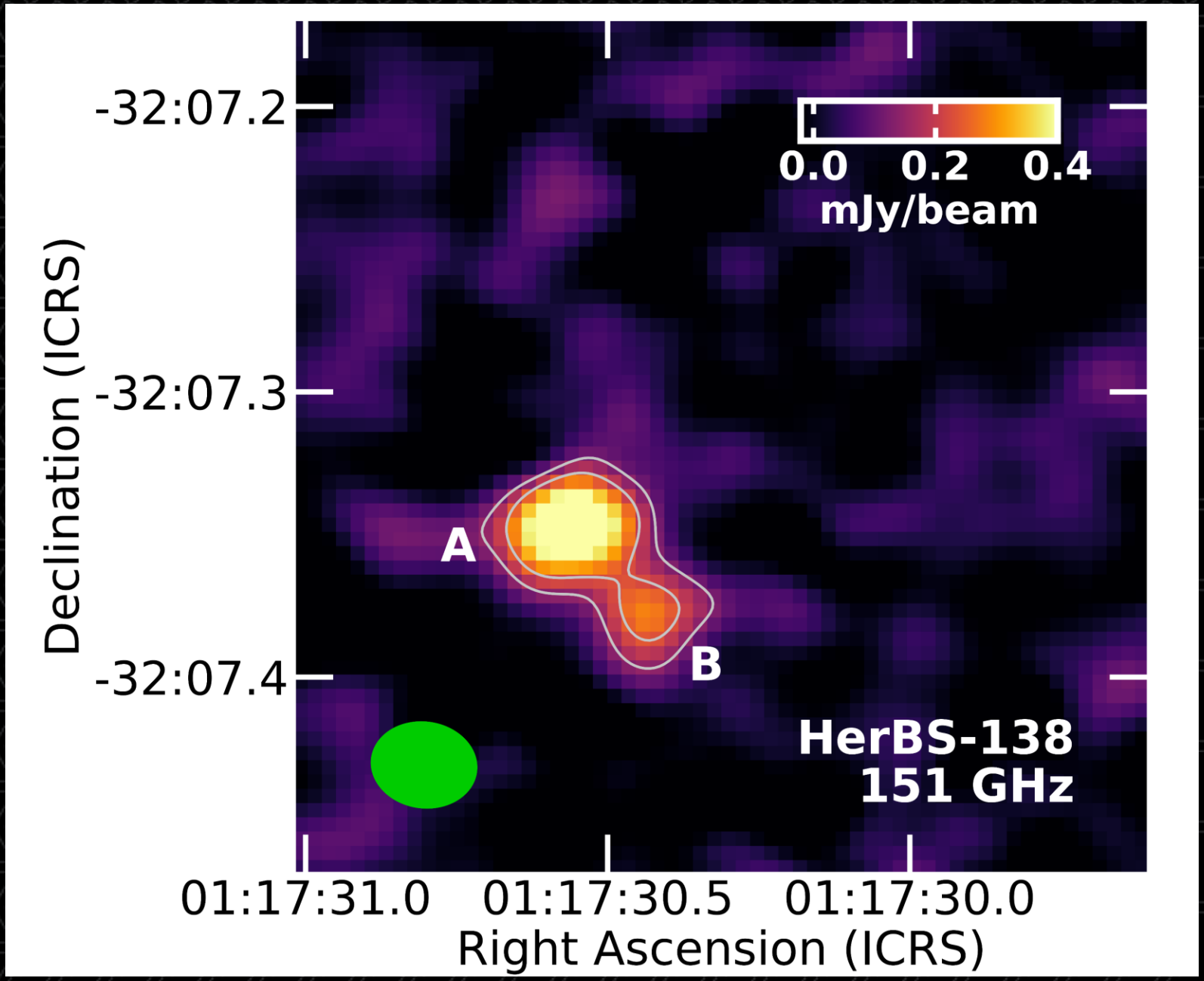
-32:07.2
-32:07.3
-32:07.4
Declination (ICRS)
0.0
0.2
0.4
mJy/beam
A
B
HerBS-138
151 GHz
01:17:31.0
01:17:30.5
01:17:30.0
Right Ascension (ICRS)

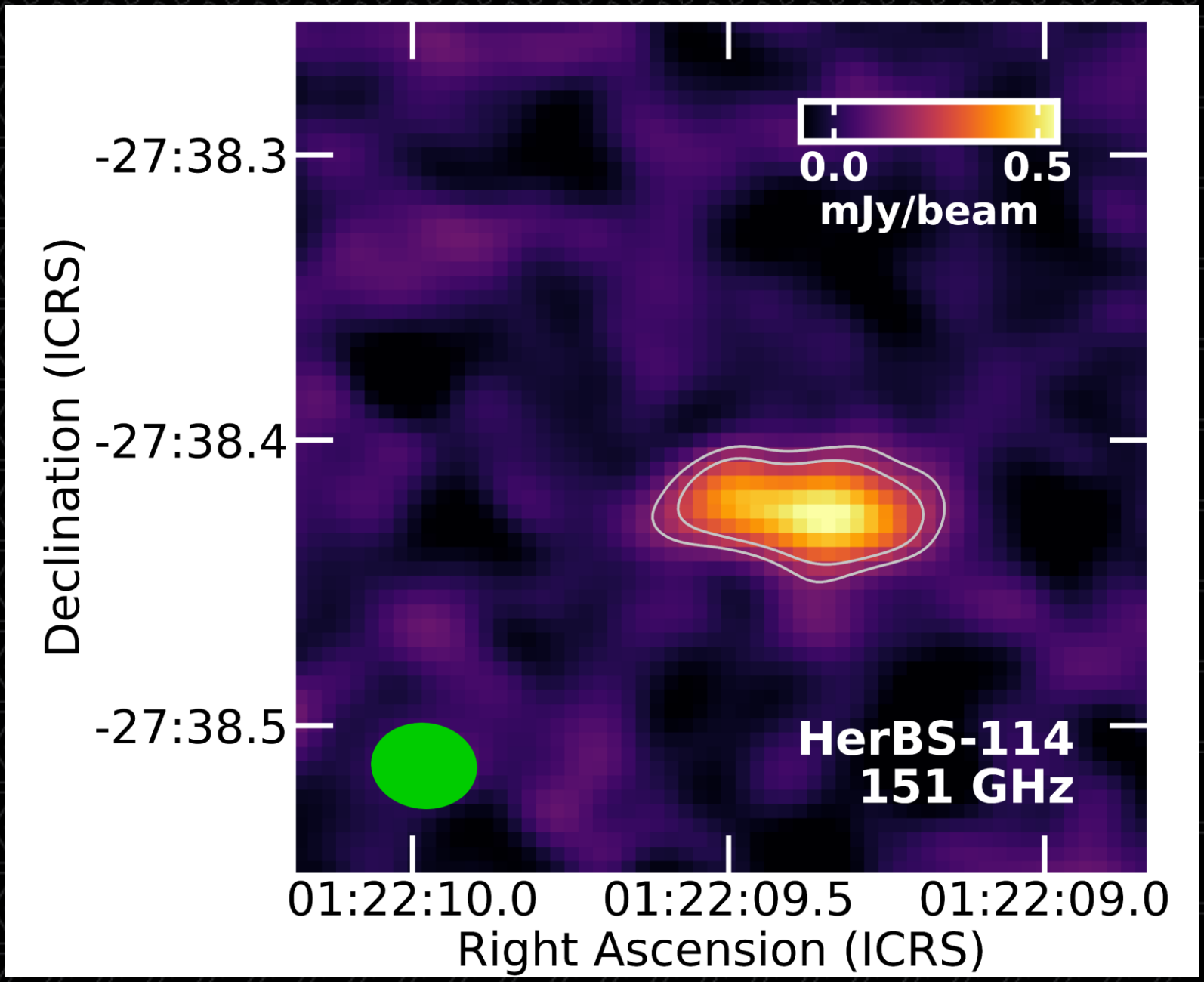
-27:38.3
-27:38.4
-27:38.5
Declination (ICRS)
0.0
0.5
mJy/beam
HerBS-114
151 GHz
01:22:10.0
01:22:09.5
01:22:09.0
Right Ascension (ICRS)

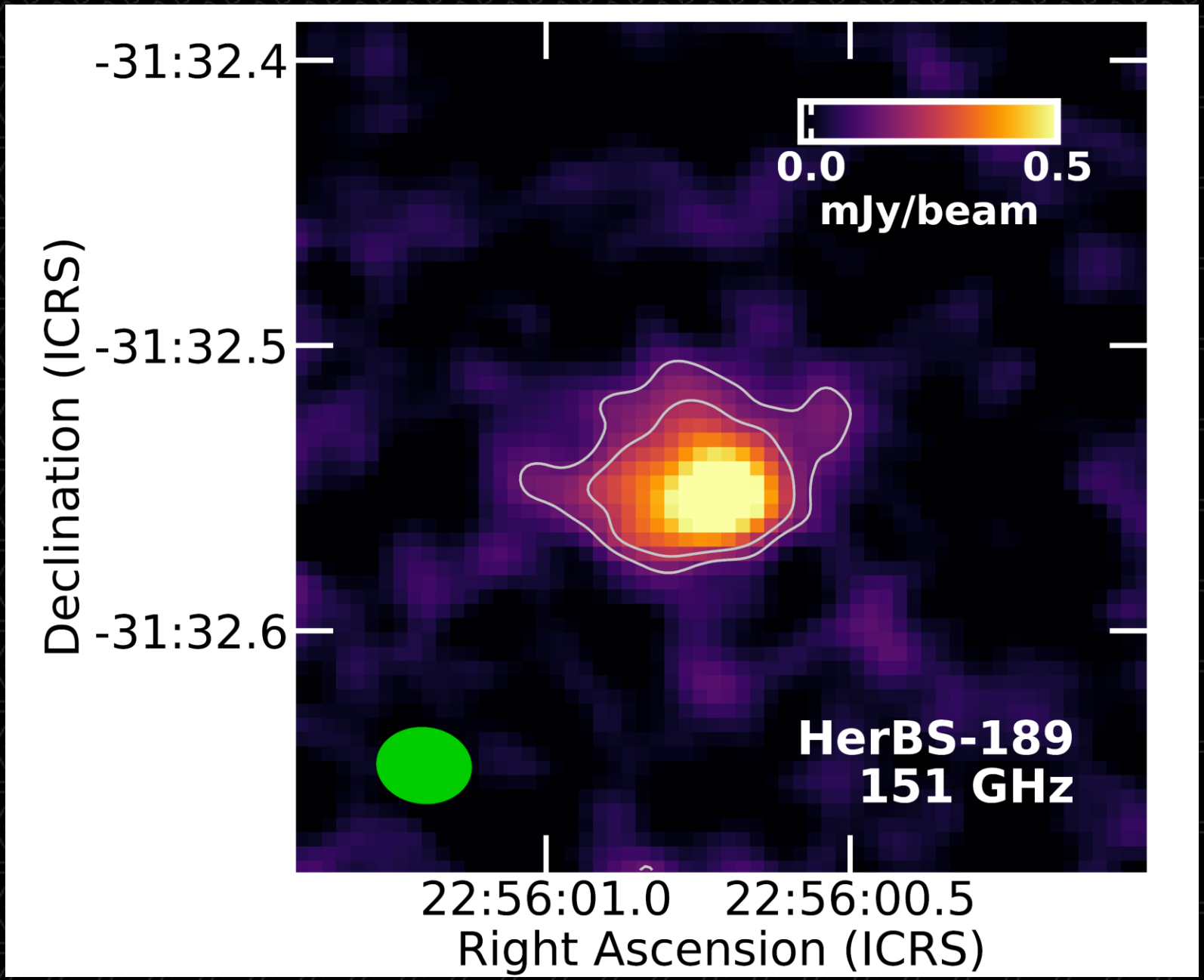
-31:32.4
-31:32.5
-31:32.6
Declination (ICRS)
0.0
0.5
mJy/beam
HerBS-189
151 GHz
22:56:01.0
22:56:00.5
Right Ascension (ICRS)

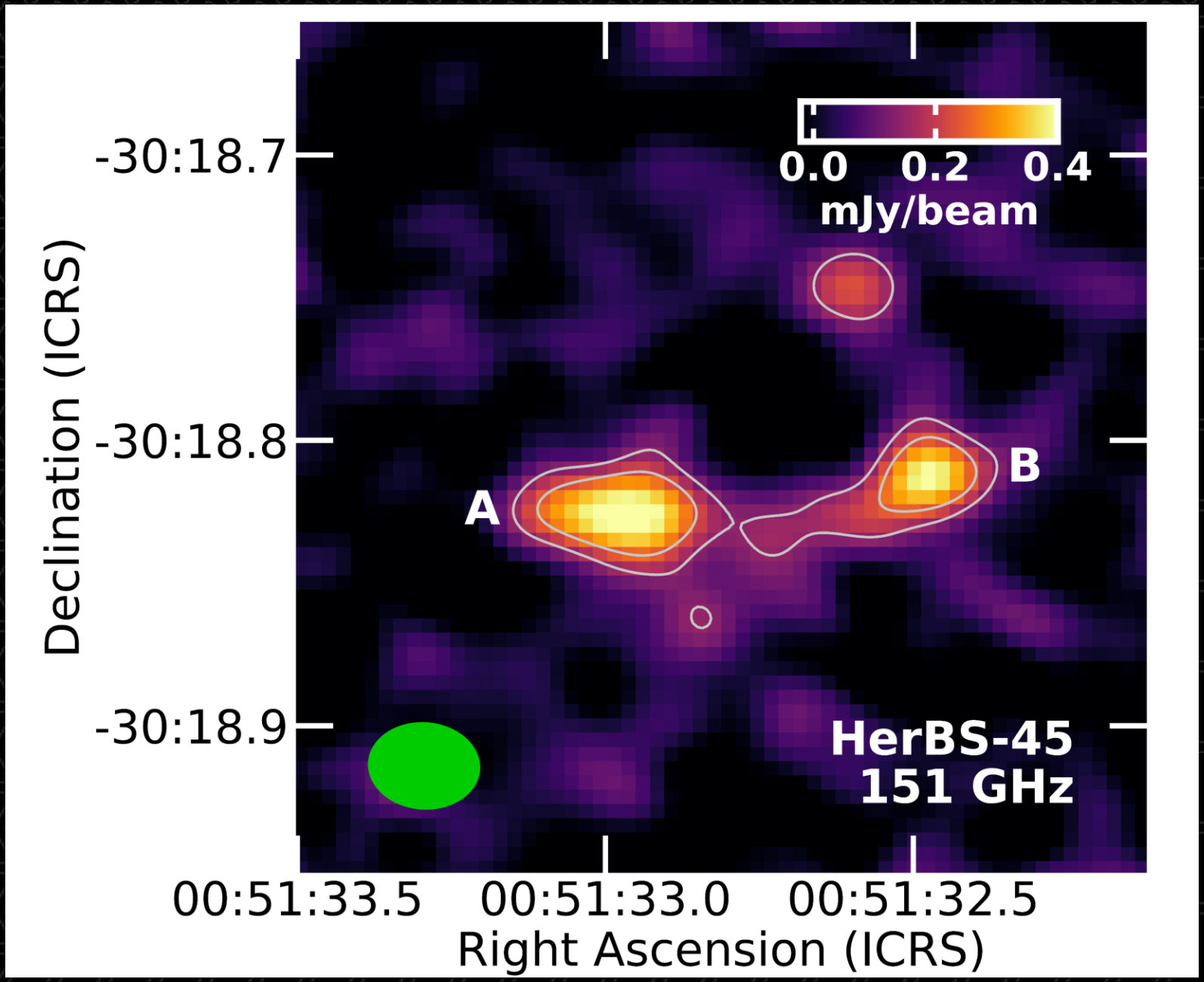
-30:18.7
-30:18.8
-30:18.9
Declination (ICRS)
0.0
0.2
0.4
mJy/beam
A
B
HerBS-45
151 GHz
00:51:33.5
00:51:33.0
00:51:32.5
Right Ascension (ICRS)

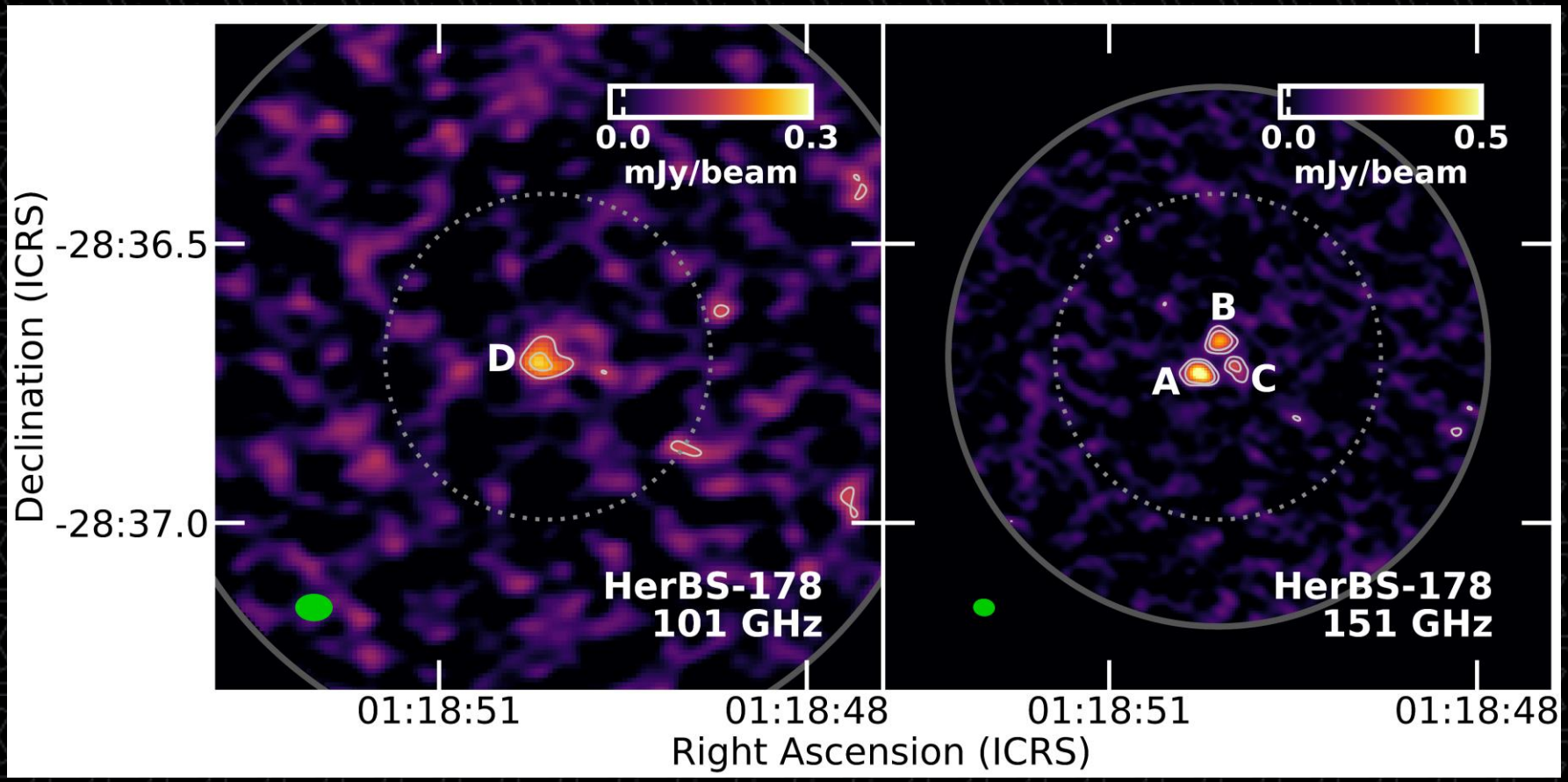
0.0
0.3
mJy/beam
D
HerBS-178
101 GHz
0.0
0.5
mJy/beam
B
A
C
HerBS-178
151 GHz
Declination (ICRS)
-28:36.5
-28:37.0
01:18:51
01:18:48
01:18:51
01:18:48
Right Ascension (ICRS)

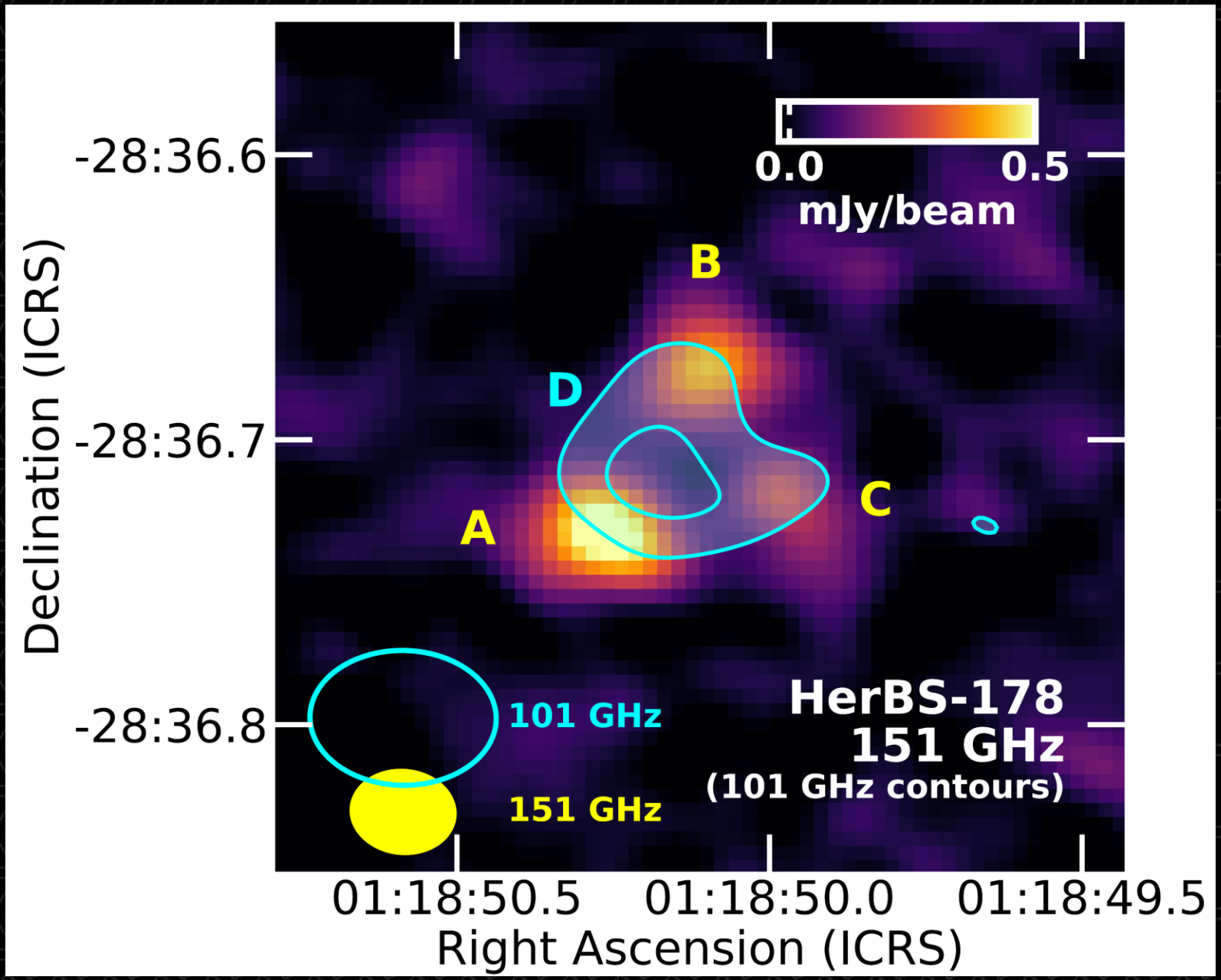
0.0
0.5
mJy/beam
B
D
C
A
101 GHz
151 GHz
HerBS-178
151 GHz
(101 GHz contours)
-28:36.6
-28:36.7
-28:36.8
Declination (ICRS)
01:18:50.5
01:18:50.0
01:18:49.5
Right Ascension (ICRS)

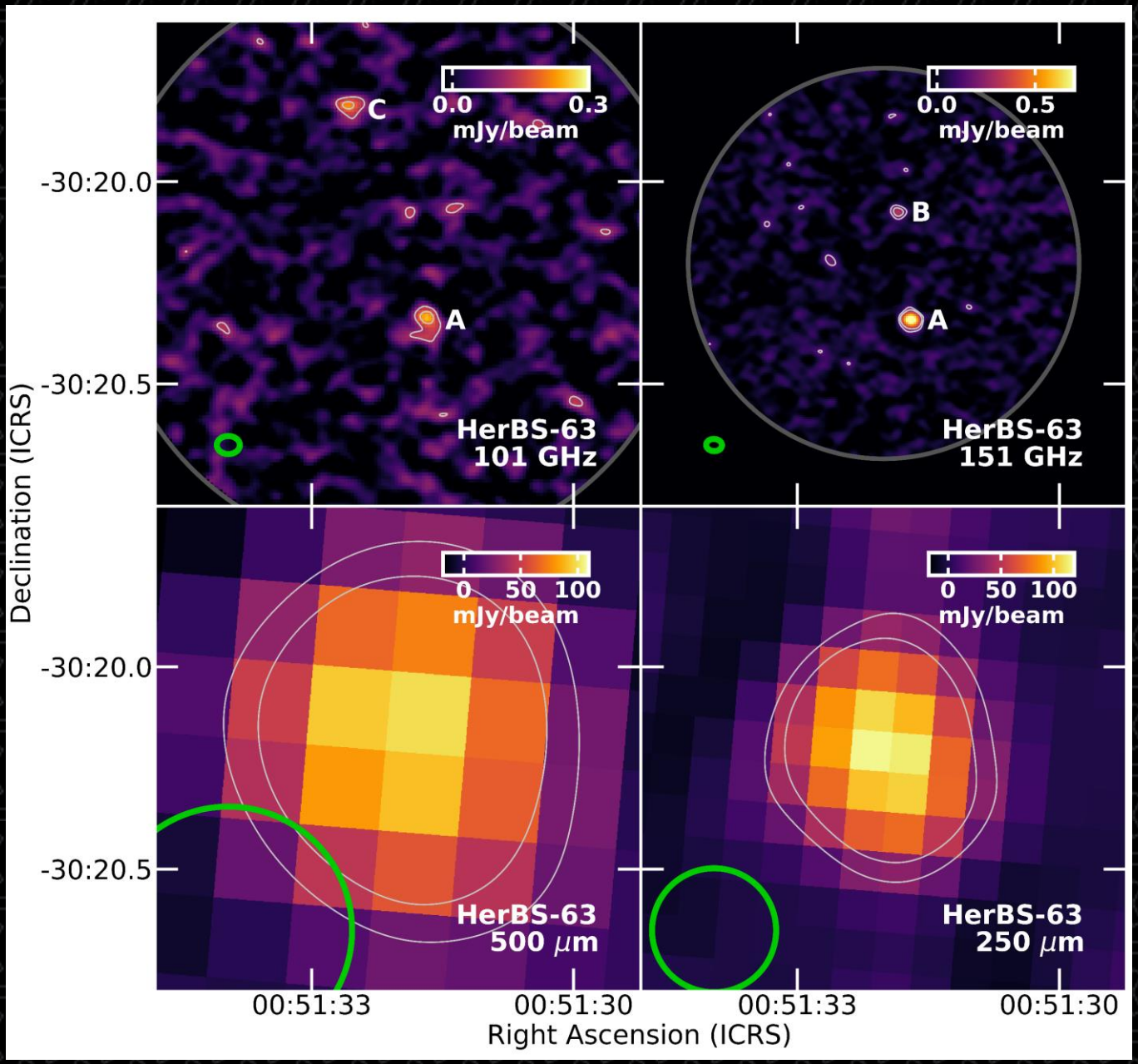
C
0.0
0.3
mJy/beam
HerBS-63
101 GHz
B
A
0.0
0.5
mJy/beam
HerBS-63
151 GHz
0
50
100
mJy/beam
HerBS-63
500 μm
0
50
100
mJy/beam
HerBS-63
250 μm
-30:20.0
-30:20.5
-30:20.0
-30:20.5
Declination (ICRS)
00:51:33
00:51:30
00:51:33
00:51:30
Right Ascension (ICRS)

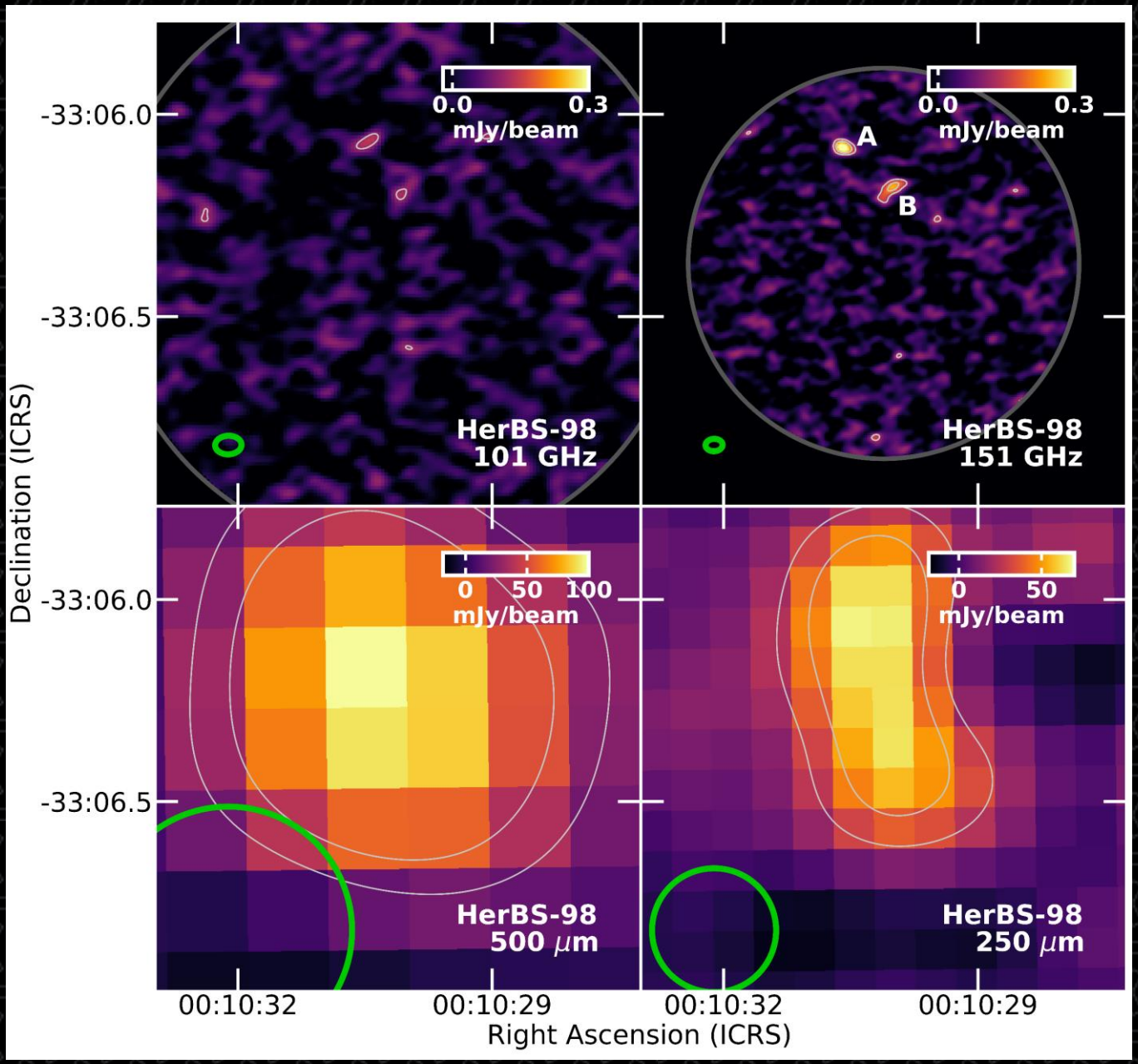
-33:06.0
-33:06.5
Declination (ICRS)
0.0
0.3
mJy/beam
A
B
HerBS-98
101 GHz
HerBS-98
151 GHz
0
50
100
HerBS-98
500 μm
HerBS-98
250 μm
00:10:32
00:10:29
Right Ascension (ICRS)

These data looked immediately useful for studying multiplicities (how sources detected by single-dish telescopes like Herschel are resolved into multiple sources by interferometers like ALMA).

Number of detected sources within ALMA field	Number of ALMA fields
1	39
2	34
≥3	7
At least one detected source outside the central 35"	6

About 50% (39/85) of the fields contained single sources in the ALMA data (with angular resolutions of 2”).

Number of detected sources within ALMA field	Number of ALMA fields
1	39
2	34
≥3	7
At least one detected source outside the central 35"	6

Slightly fewer (34/85) of the fields contained two sources.

Only 6 of these pairs of sources had the same measured spectroscopic redshift.

6 of the sources had different measured spectroscopic redshifts.

Number of detected sources within ALMA field	Number of ALMA fields
1	39
2	34
≥3	7
At least one detected source outside the central 35"	6

6/85 fields had three or more sources. We never found a case where all sources had the same redshift.

Number of detected sources within ALMA field	Number of ALMA fields
1	39
2	34
≥3	7
At least one detected source outside the central 35"	6

6/85 fields had a detected source that fell outside the beam of the Herschel data.

The interpretation of these data for multiplicities was unclear, so these fields were not included in the rest of the analysis.

Number of detected sources within ALMA field	Number of ALMA fields
1	39
2	34
≥3	7
At least one detected source outside the central 35"	6

When two sources were detected in ALMA data, it was typically the case that the second source contributed a significant fraction of the total emission.

When three or more sources were detected in ALMA data, the brightest source typically contributed a small fraction of the total emission.

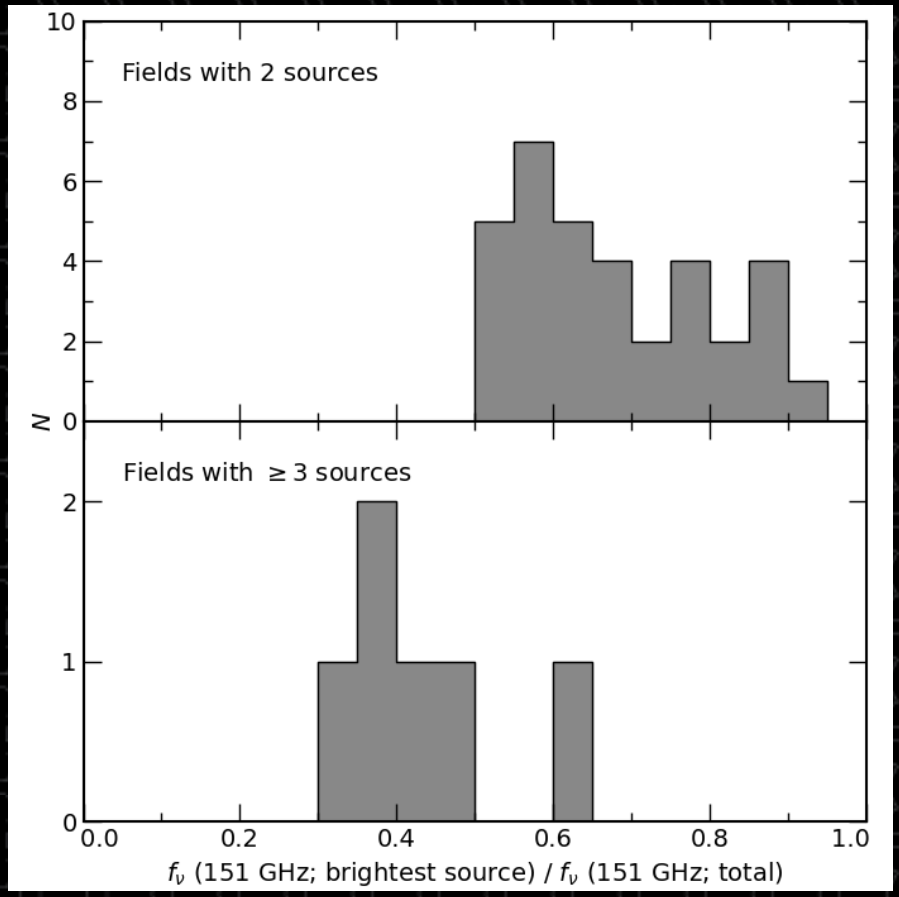

The brightest fields tended to contain single sources (probably bright, unresolved gravitational lenses).

No other notable trends were seen in terms of multiplicity versus the total emission in the field.

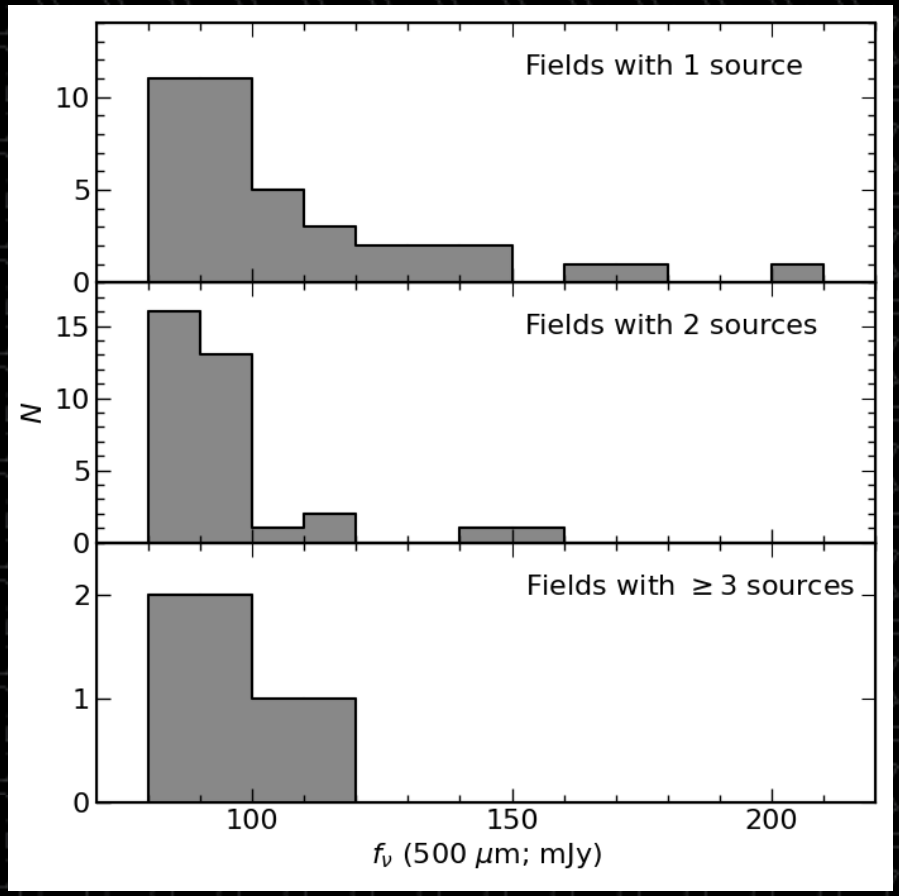

The brightest fields tended to contain single sources (probably bright, unresolved gravitational lenses).

No other notable trends were seen in terms of multiplicity versus the total emission in the field.

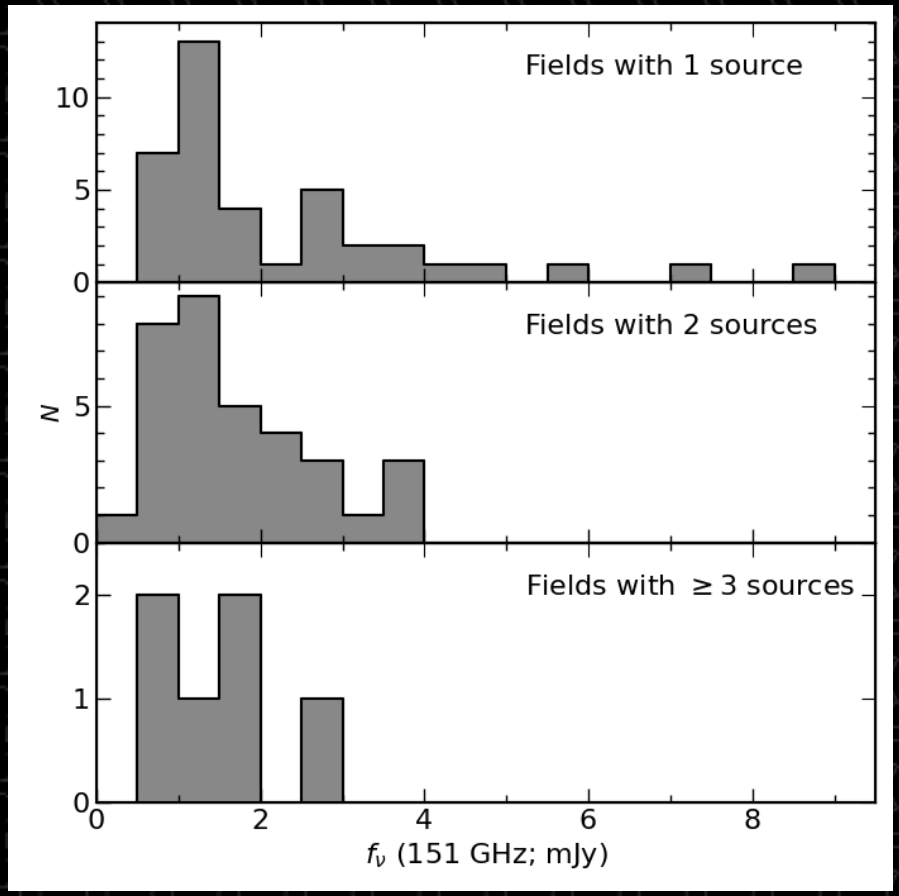

Compared to previously-published results, the BEARS data fall within the midrange of the fraction of fields that contain multiple sources.

These results depend on multiple factors:

- Sample selection.
- Beam/wavelength used for the original observations.
- Beam/wavelength used for follow-up observations.
- Sensitivity levels.
- How sources were counted.

Reference	Percentage of fields found to contain multiple sources
Stach et al. (2018)	11 %
Cowie et al. (2018)	13 %
Hill et al. (2018)	≤15 %
Hodge et al. (2013)	35-50 %
Bendo et al. (2023)	***49 %***
Bussmann et al. (2015)	69 %
Hayward et al. (2013)	82 %
Scudder et al. (2018)	93 %

We also tended to find many single sources in fields with high total flux densities.

This contradicts the results from many prior studies (Hayward et al. 2013, Hodge et al. 2013, Karim et al. 2013, Stach et al. 2018).

Reference	Percentage of fields found to contain multiple sources
Stach et al. (2018)	11 %
Cowie et al. (2018)	13 %
Hill et al. (2018)	≤15 %
Hodge et al. (2013)	35-50 %
Bendo et al. (2023)	***49 %***
Bussmann et al. (2015)	69 %
Hayward et al. (2013)	82 %
Scudder et al. (2018)	93 %

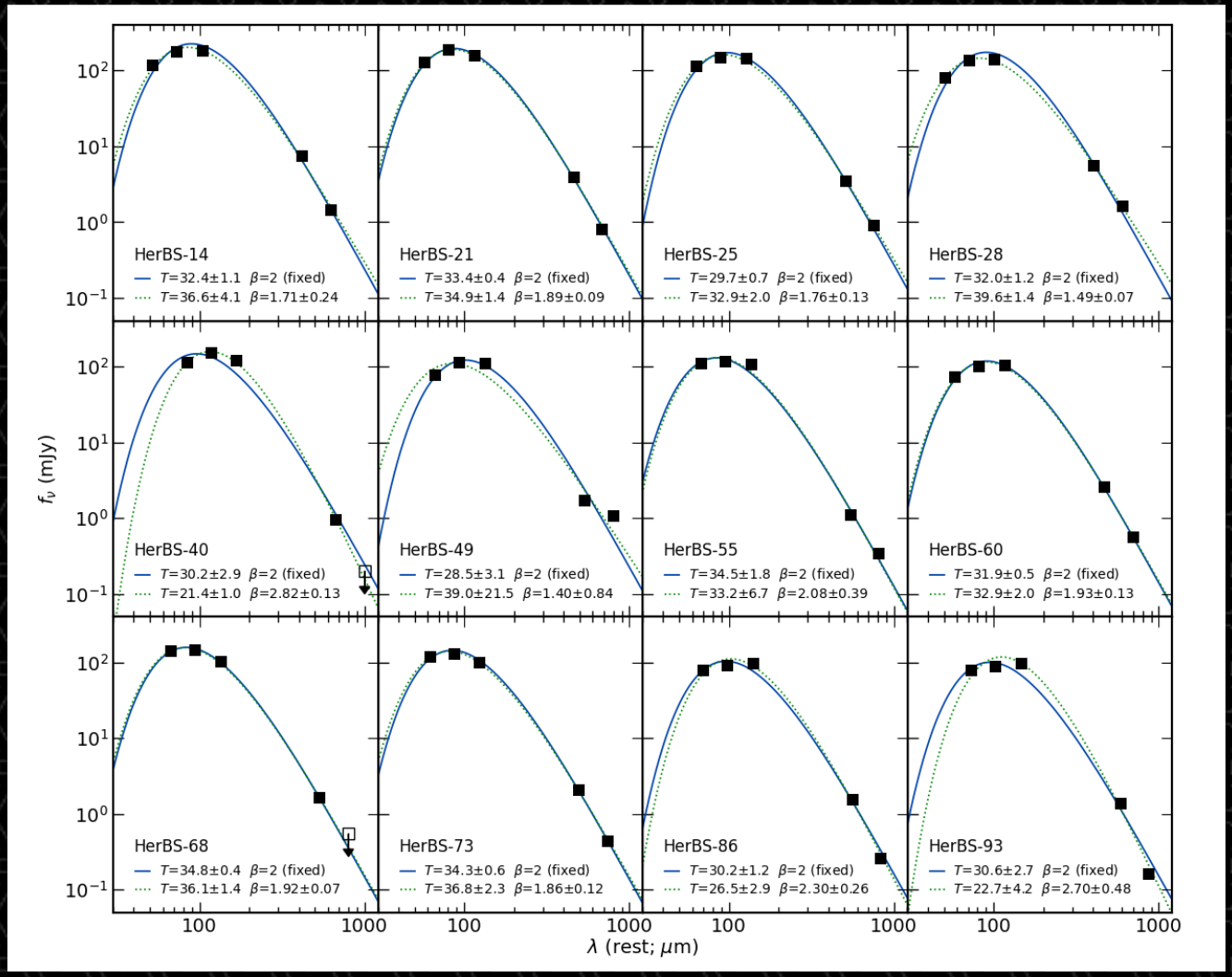

For fields that contained one source or two sources at the same spectroscopic redshift, we could combine the Herschel and ALMA data to create SEDs.

The SED fits provided one set of measurements of the dust emissivity index β.

The 151/101 GHz ratios from ALMA provided a different way of measuring β.

The two results do not agree.

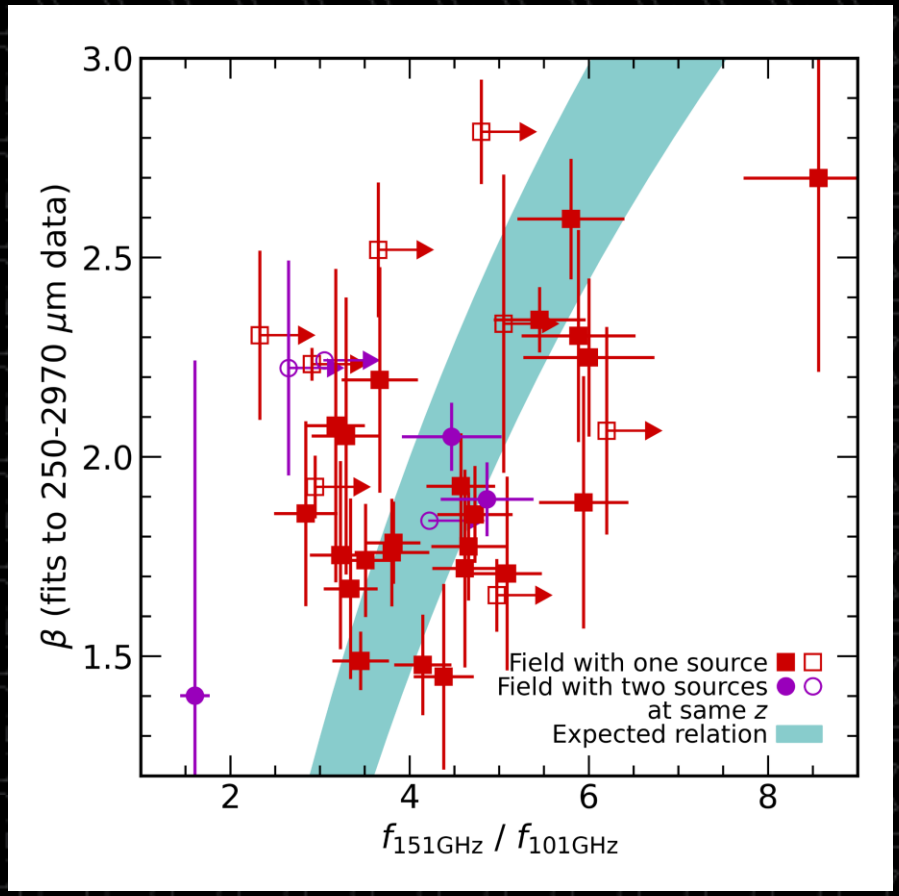

When β was treated as a free parameter, temperature varied with β (a known degeneracy issue with SED fitting).

The 151/101 GHz ratios do not vary with temperature.

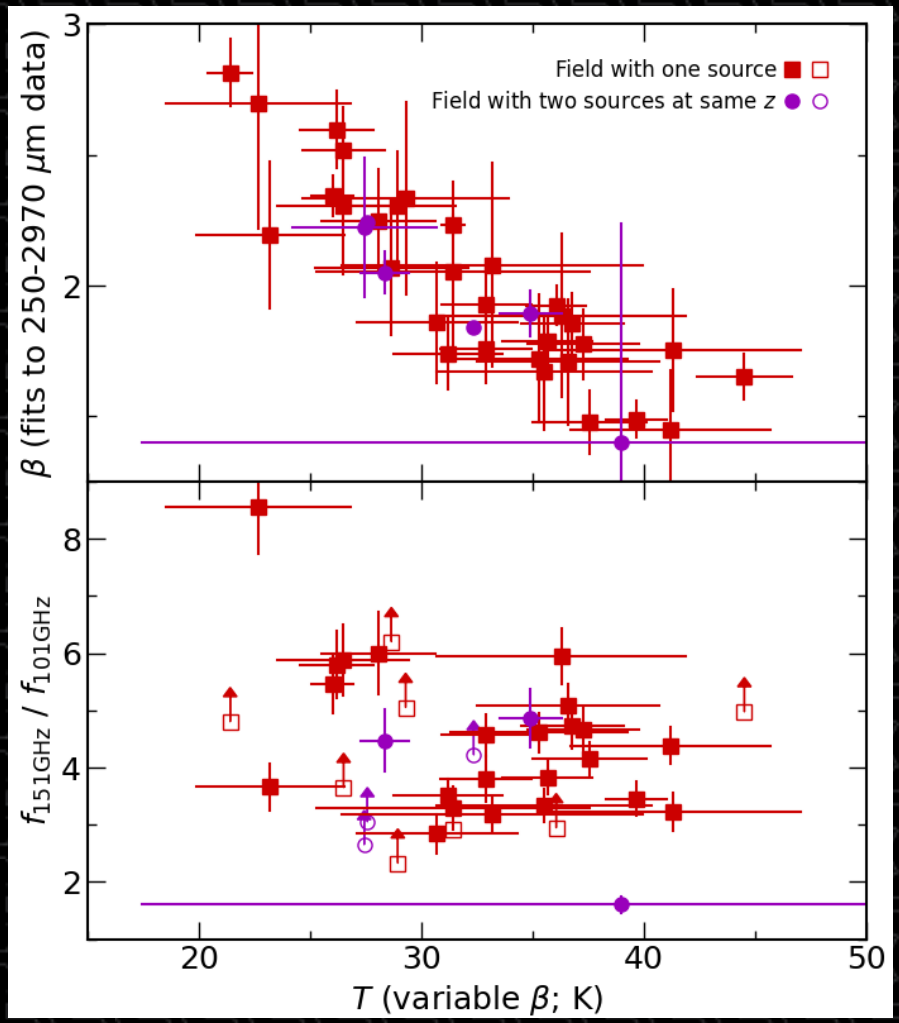

Additionally, β was found to vary with redshift when it was treated as a free parameter.

The 151/101 GHz ratios do not vary with redshift.

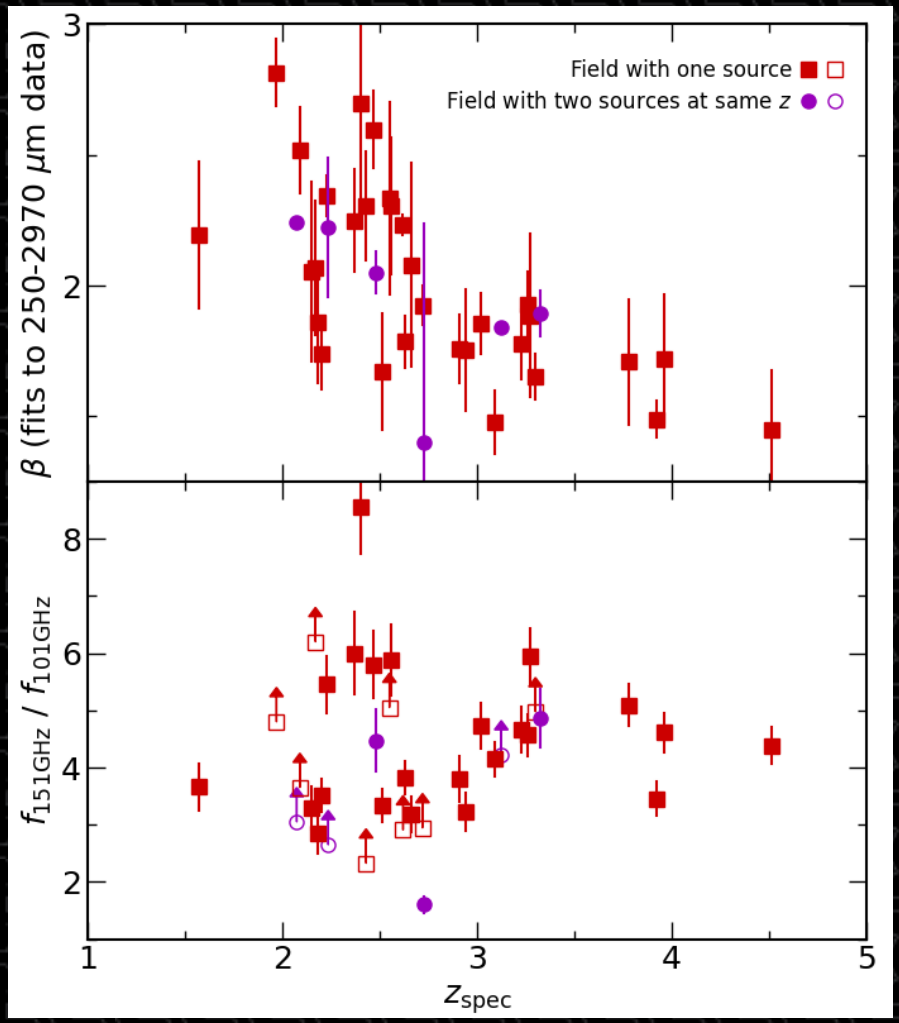

This ultimately points to issues with the SED fits with variable β. It looks like these SEDs cover dust emission from dust at multiple temperatures.

When shifting to higher redshift, shorter frequencies would sample dust at higher temperatures, thus making the peak look broader (and making the best fitting β lower).

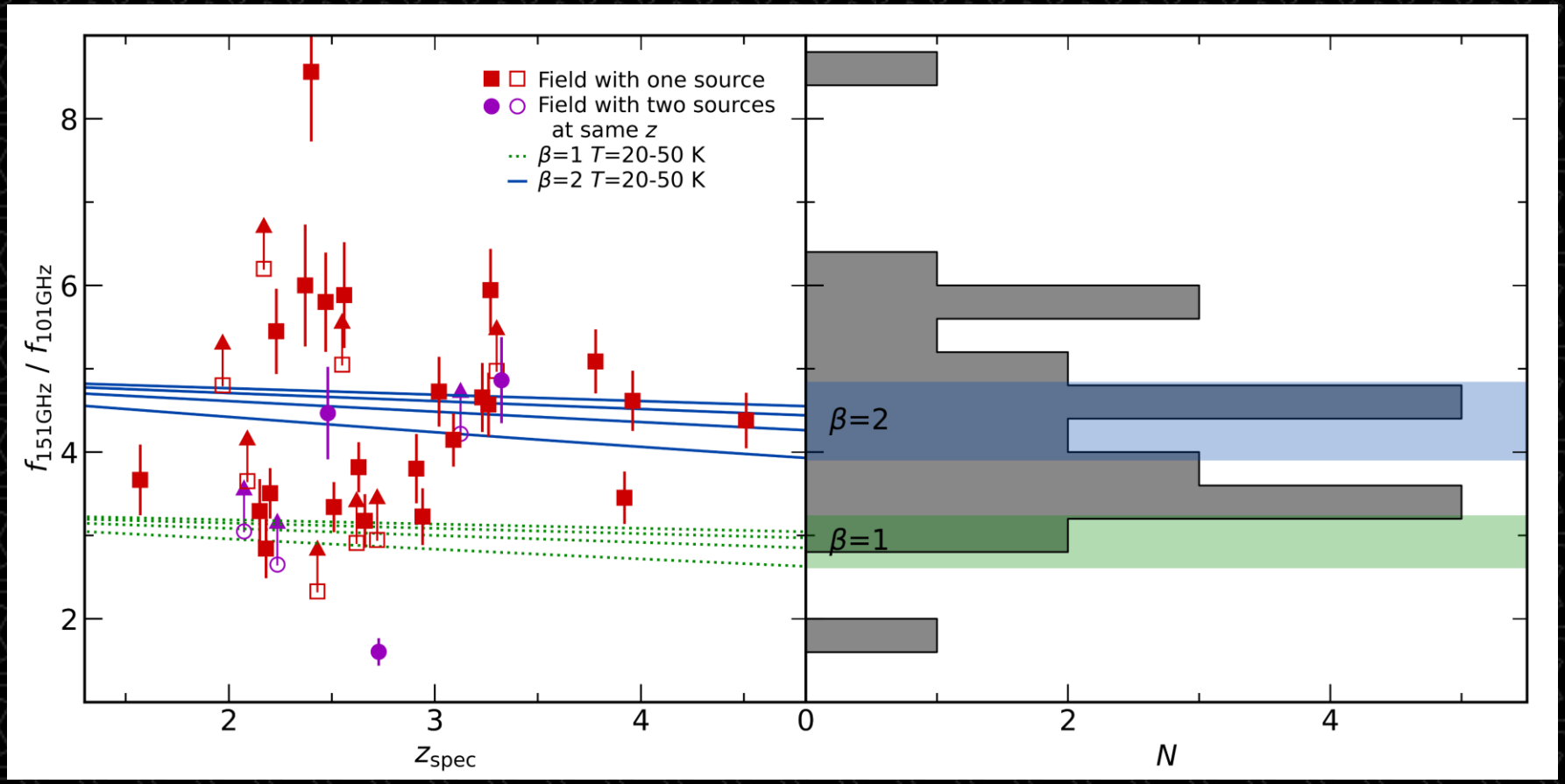

The 151/101 GHz ratios were largely consistent with β = 2, although some variations are seen in these ratios. Low ratios would be consistent with the presence of synchrotron emission from AGN, but higher ratios are much harder to explain.

We continued our analysis using SED fits based on SED fits where β was fixed to 2.

The colour temperatures from our data show only a weak dependence on redshift (correlation coefficient of 0.39).

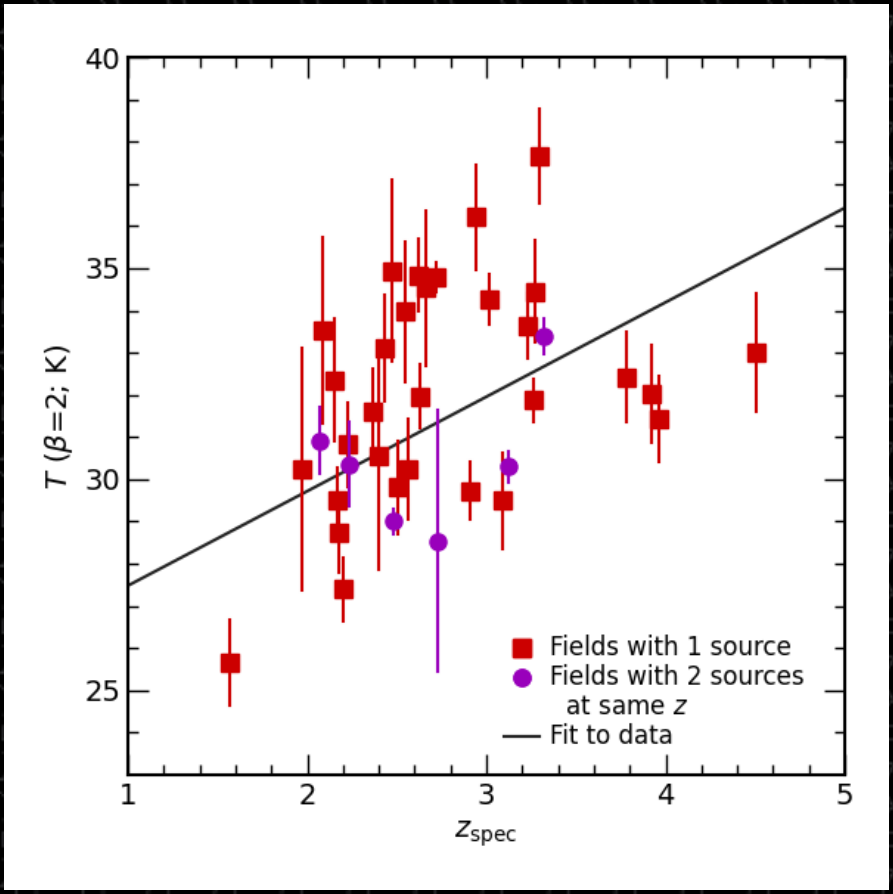

Some other analyses had found much stronger relations between colour temperature and redshift.

Others found weak or no relations between these quantities.

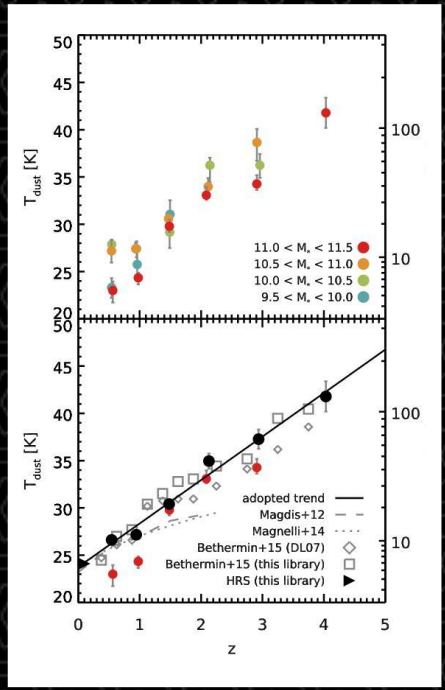

Schreiber et al. (2018, A&A, 609, A30)

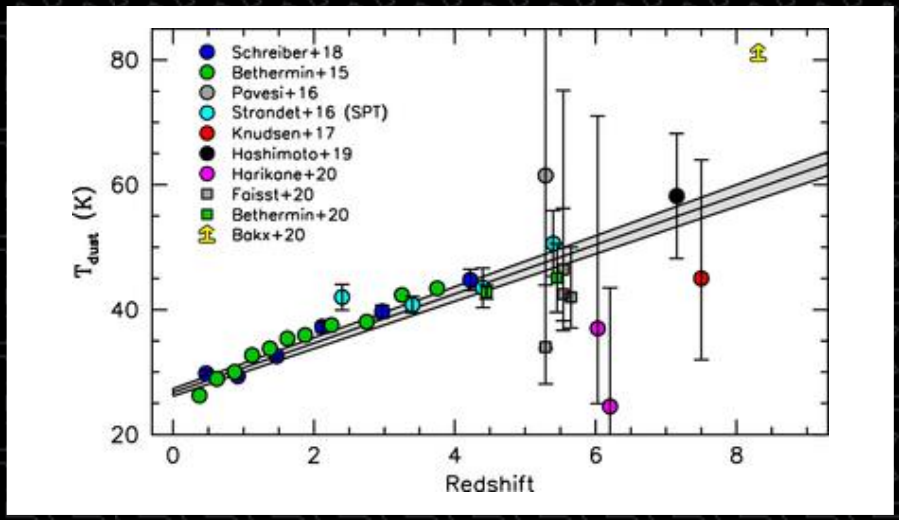

Bouwens et al. (2020, ApJ, 902, 112)

Some other analyses had found much stronger relations between colour temperature and redshift.

Others found weak or no relations between these quantities.

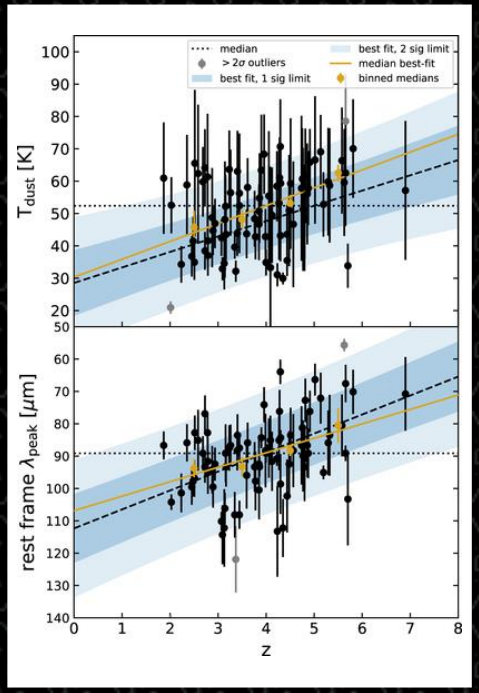

Reuter et al. (2020, ApJ, 902, 78)

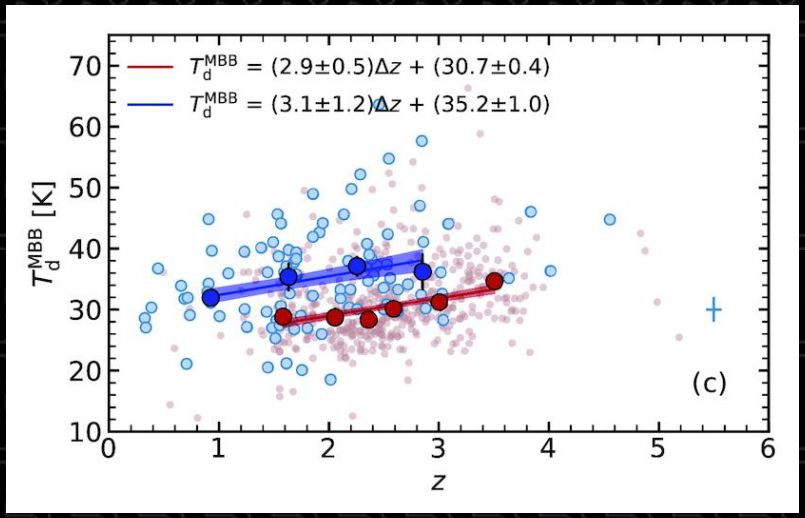

Dudzeviciute et al. (2021, MNRAS, 500, 942)

The differences in these results look related to selection effects.

Optical/near-infrared samples show strong relations. These tend to be main sequence galaxies.

Far-infrared/submillimetre samples show no relation. These tend to be more extreme starbursts.

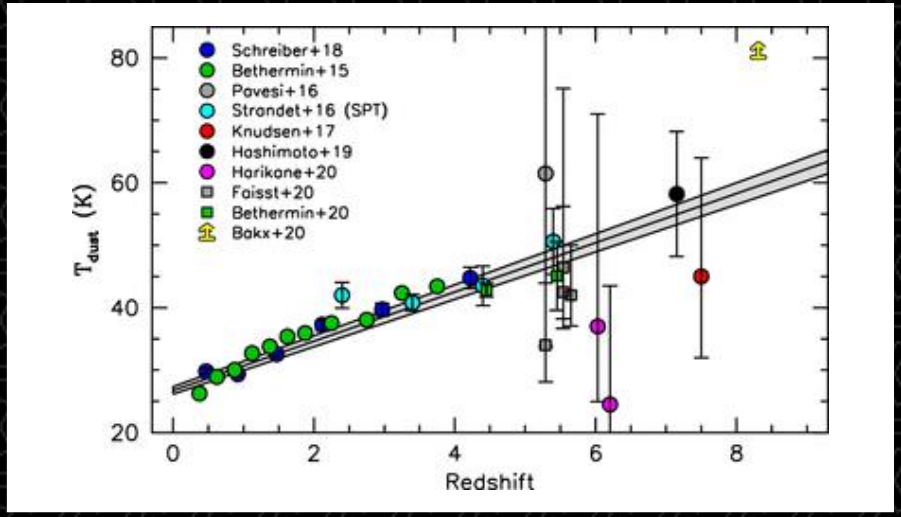

Bouwens et al. (2020, ApJ, 902, 112)

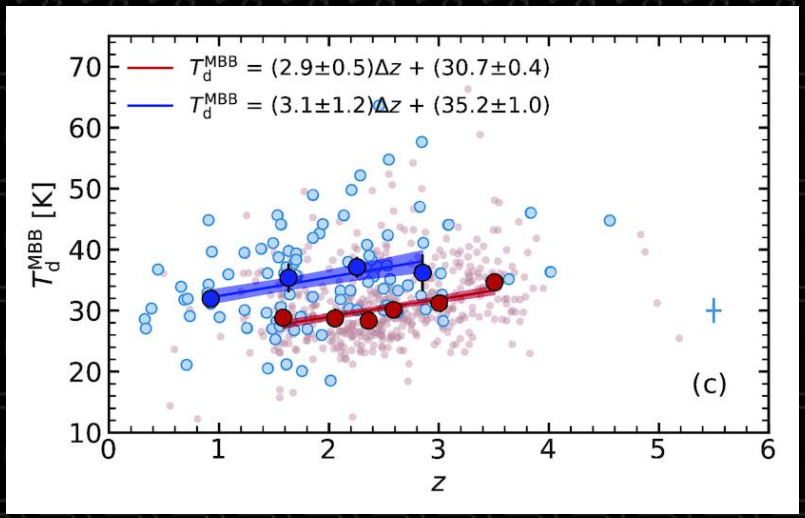

Dudzeviciute et al. (2021, MNRAS, 500, 942)

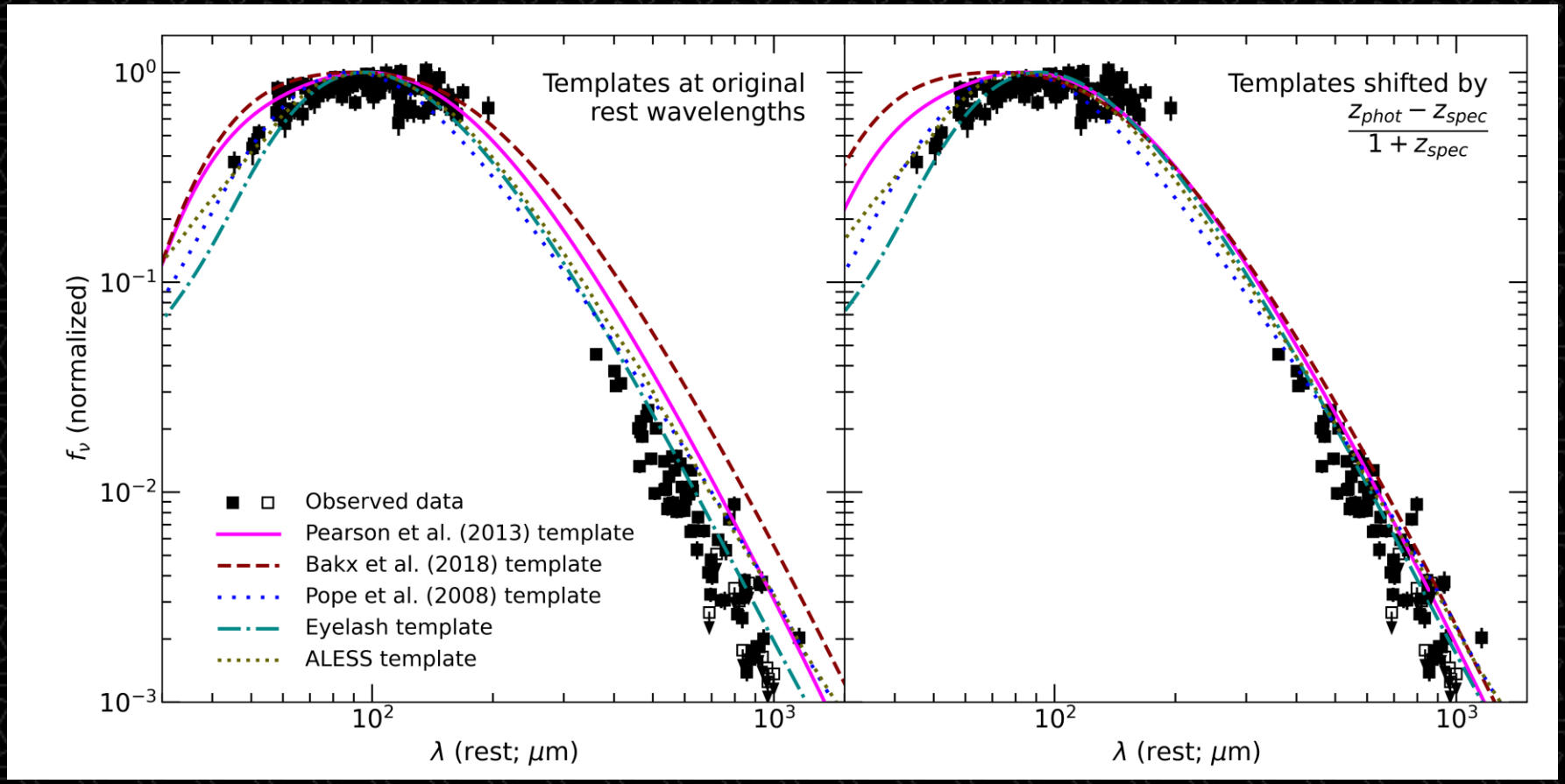

We also tested how photometric redshifts from various popular SED templates compared to our spectroscopic redshifts. The photometric redshifts were systematically low.

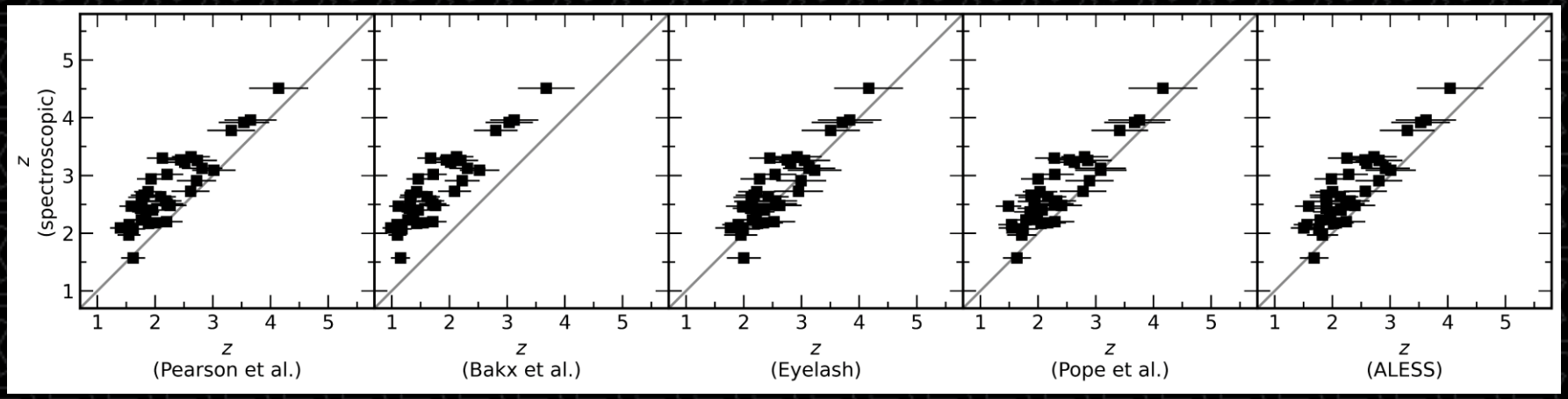

We also tested how photometric redshifts from various popular SED templates compared to our spectroscopic redshifts. The photometric redshifts were systematically low.

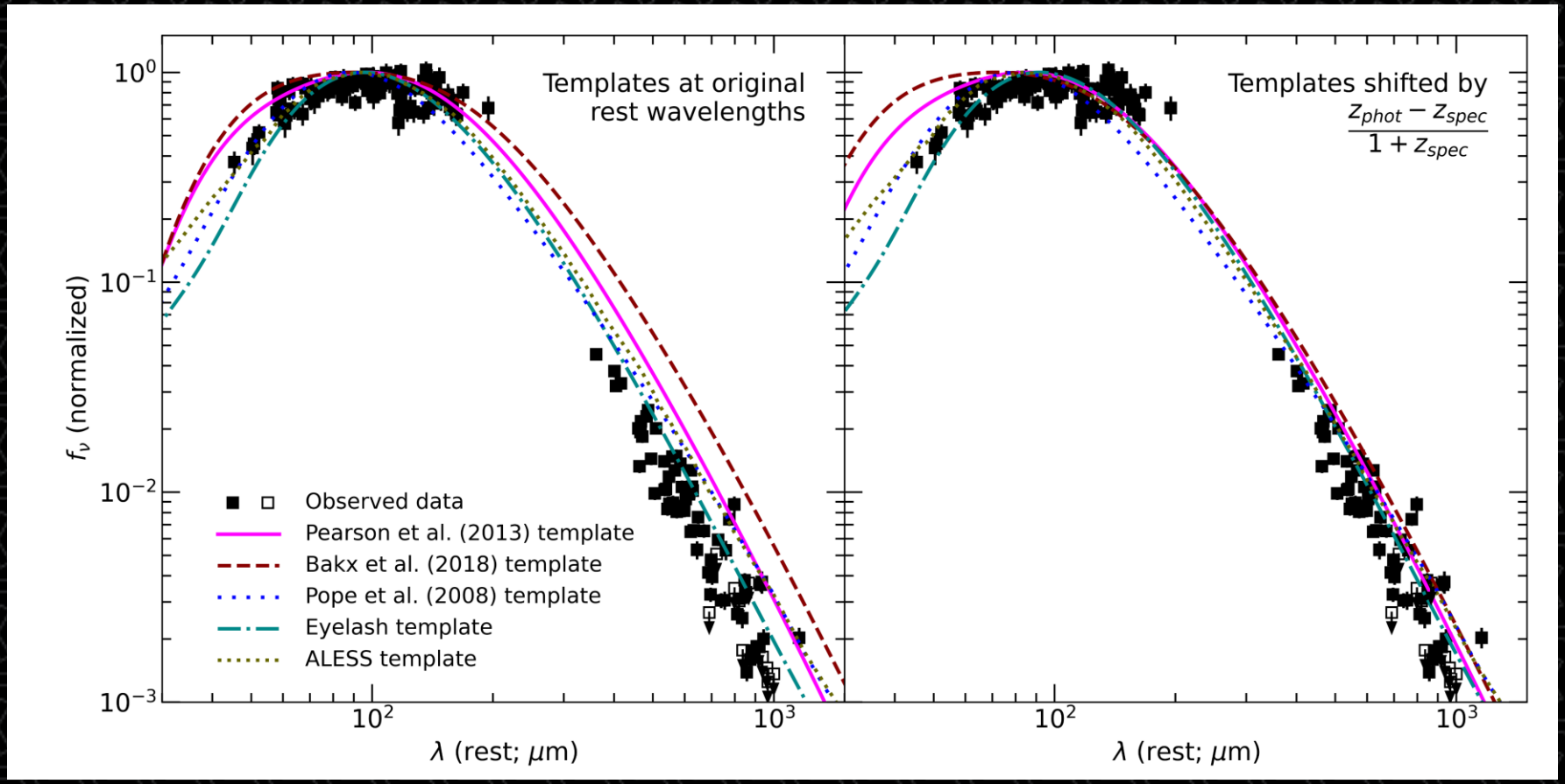

The main problem seems to be that the templates are based on dust with cooler temperatures than what we measured. Additionally, some SED templates had broader peaks than the SEDs that we measured.

Conclusions

- The BEARS fields yielded many potential gravitational lens objects, but the fields also contain many other types of objects.
- The multiplicity results for BEARS falls within the midrange of what has previously been measured (but this depends on multiple factors).
- The 151/101 GHz ratios yield a dust emissivity index β equal to 2. This is one of the very few measurements of β in $z>1$ objects.
- Dust temperatures in the gravitational lens candidates do not vary strongly with redshift, which is consistent with other objects selected at far-infrared or submillimetre wavelengths.
- The SED templates we tested typically gave redshifts ~15% lower than the spectroscopic redshifts.

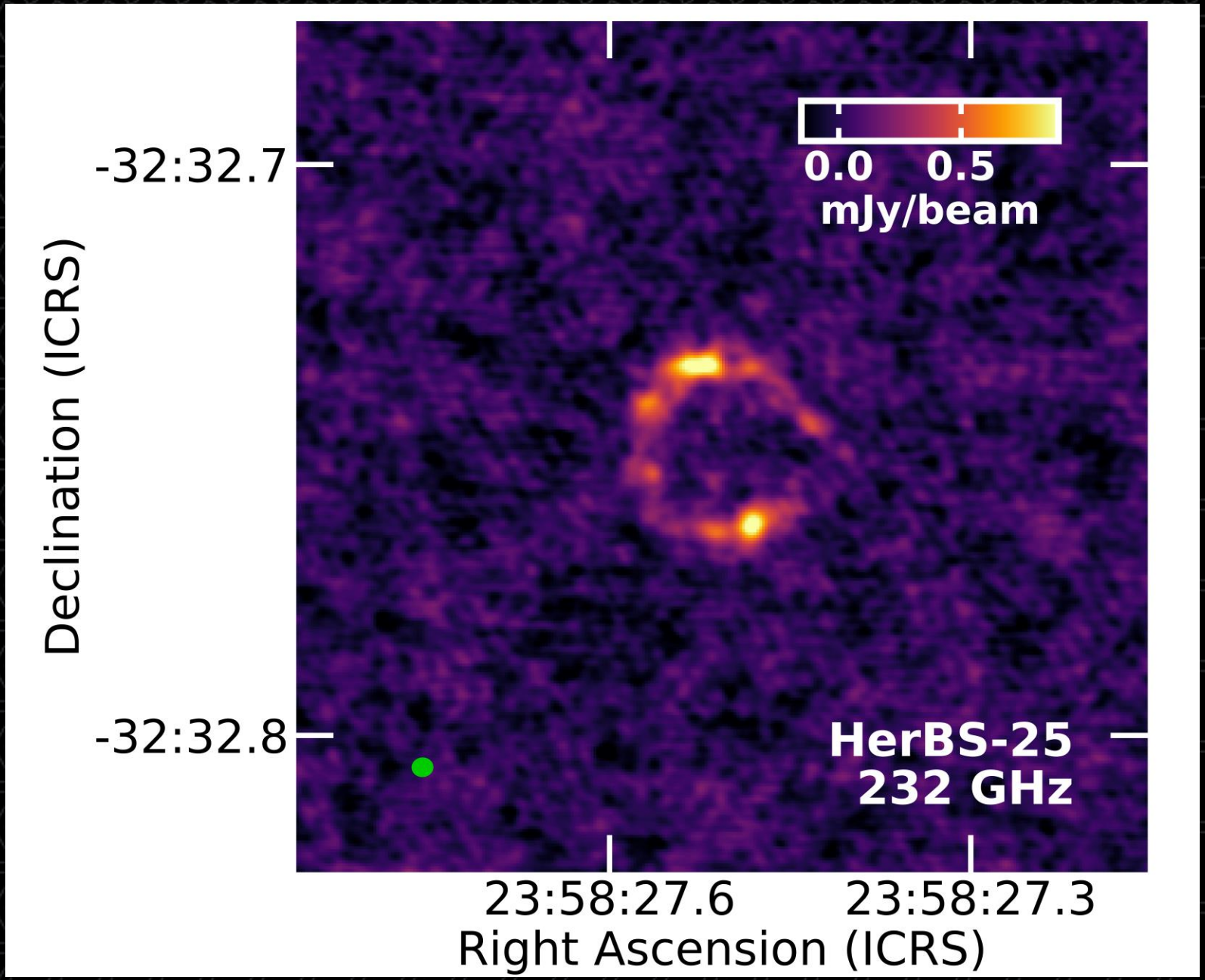
-32:32.7
-32:32.8
Declination (ICRS)
0.0
0.5
mJy/beam
HerBS-25
232 GHz
23:58:27.6
23:58:27.3
Right Ascension (ICRS)

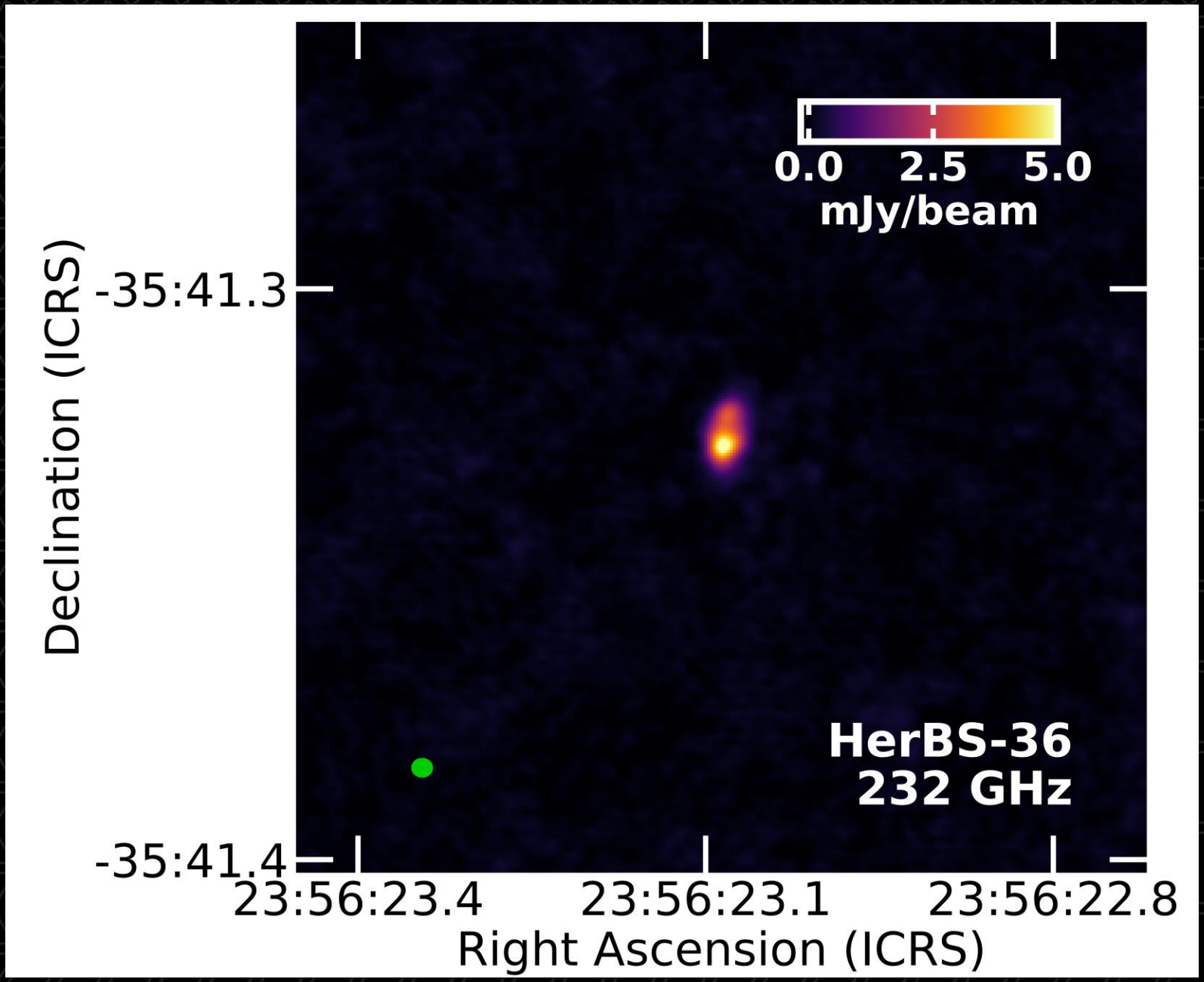
0.0
2.5
5.0
mJy/beam
HerBS-36
232 GHz
-35:41.3
-35:41.4
Declination (ICRS)
23:56:23.4
23:56:23.1
23:56:22.8
Right Ascension (ICRS)

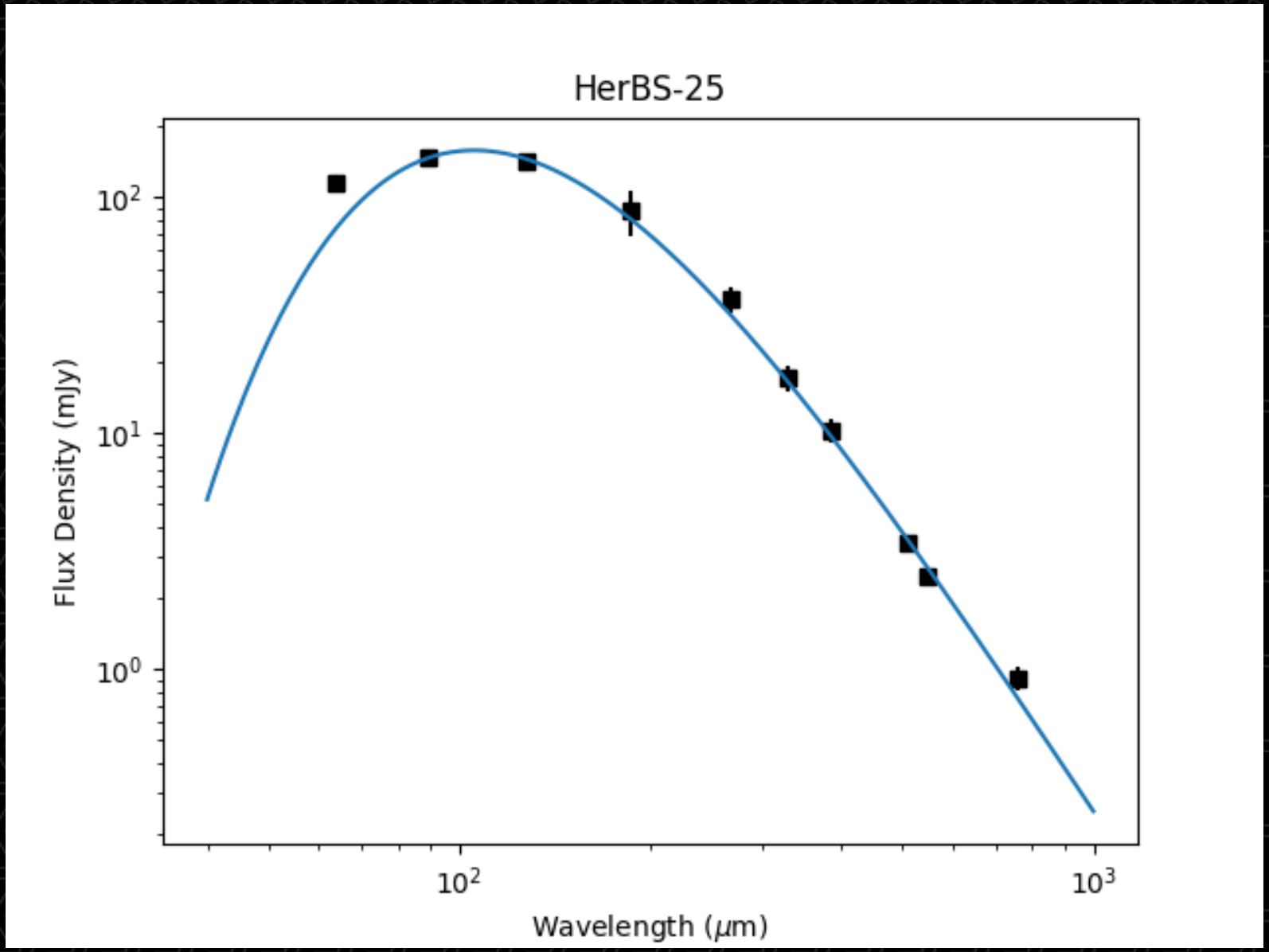
HerBS-25
Flux Density (mJy)
10^2
10^1
10^0
10^2
10^3
Wavelength (μm)

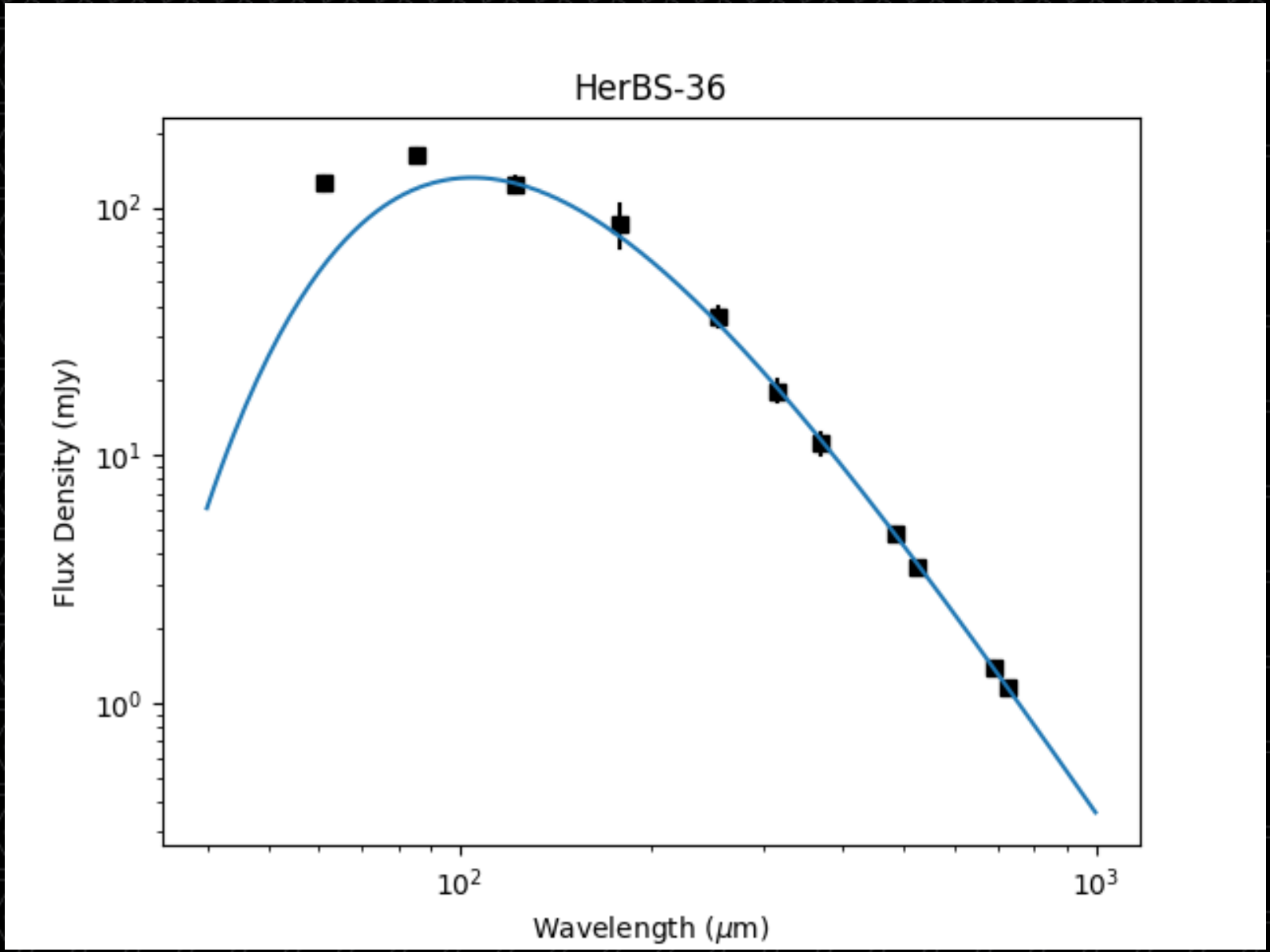
HerBS-36
Flux Density (mJy)
10^2
10^1
10^0
10^2
10^3
Wavelength (μm)